The Wave Dissipation Potential of *Spartina alterniflora* in the Bay of Fundy

Honours Thesis: Environmental Science

Makadunyiswe D. Ngulube

Supervisor: Dr. Danika van Proosdij

The Wave Dissipation Potential of *Spartina alterniflora* in the Bay of Fundy

By Makadunyiswe D. Ngulube

ABSTRACT

The purpose of this research is to determine the wave dissipation potential of salt marsh vegetation in a temperate, hypertidal estuary. The study site is Clifton Marsh, Nova Scotia, in the Bay of Fundy. This site was selected in part because it is monospecific, with *Spartina alterniflora*. This research will investigate how effective *Spartina alterniflora* is at attenuating wave energy and the variability in wave height as the vegetation height increases over time. A transect was set up with 4 RBRduet3 T.D|wave16 — temperature and pressure loggers extending from the mudflat to the vegetated section. Data were collected from mid June to early December 2020. For each two-week dataset, the data was sorted to include only that with a depth greater than 0.1 m, and events were selected to have a significant wave height that is greater than 0.05 m. Vegetation surveys were carried out bi-weekly to measure the various parameters such as the stem height, stem diameter and the width of the middle top parts of the leaves. The outcomes show that vegetation has an effect on the wave energy and significant wave height and affects the attenuation capacity of salt marshes. This research demonstrates that the presence of vegetation on salt marshes plays an important role in wave dissipation and attenuation. There needs to be a better understanding of vegetated intertidal environments and incoming waves, to achieve sustainable coastal management and planning.

ACKNOWLEDGMENTS

This research could not have been possible without the expert guidance and support from my supervisor, Dr. Danika van Proosdij. I am grateful for her patience throughout this project, and for her ability to constantly cheer me on, encouraging me not to take the easy way out. I am also thankful for the support of the In_CoaST team: Emma Poirier, Sade Hanley, Brandon Champagne, Élise Rogers and Megan Elliott. Finally, I would like to thank my family, the Sindah Clan, who have been extremely supportive throughout this journey. I dedicate this honours research project to you, thank you for always believing in me.

Funding for this project was provided by National Research Council (NRC), Geological Survey of Canada (GSC) which is within NRCan (Natural Resources Canada), Defence Research and Development Canada's Centre for Security Science (DRDC CSS) and NSERC ResNet.

TABLE OF CONTETS

LIST OF TABLES

LIST OF FIGURES

CHAPTER ONE

INTRODUCTION AND LITERATURE REVIEW

1. INTRODUCTION

1.1. Overview of vulnerability of coastal systems to climate change effects

Coastal systems and low-lying areas are vulnerable to climate change impacts and sea level rise (Sales, 2009). As a result, coastal communities are at risk of flooding and erosion due to rising sea levels and intensified storms (Duarte et al., 2013; Foster-Martinez et al., 2018). These vulnerable coastal areas that are under the threat of flooding and erosion, demand the implementation of sustainable measures as a means of coping with this problem (Duarte et al., 2013). It is therefore essential to address the hazards predicted by climate change and develop adaptation strategies that will ensure coastal protection (Duarte et al., 2013).

Natural hazards such as storms and hurricanes affect the coastal zone, and there has been an increase in the cost of impacts associated with these hazards (Shepard et al., 2011). Consequently, climate change effects will further exacerbate the costs of shoreline protection and impacts as the frequency and magnitude of many coastal damages will increase due to sea level rise and ocean warming (Shepard et al., 2011).

In the Maritime Provinces, large tracts of low-lying coastal lands that were former salt marshes are currently protected from tidal inundation by dykes. Intense storm surge events have been devastating in the past, overtopping existing dykes by over 0.9 m in some areas (Singh et al., 2007). Increasingly, nature-based solutions are being implemented as a response to these events (Duarte et al., 2013). Coastal ecosystems such as salt marshes, can contribute to flood risk reduction by attenuating wave energy (Vuik, 2018).

1.2. Coastal protection strategies for adaptation and mitigation

Historically, coastal protection plans have often depended upon hardened infrastructure solutions such as sea walls, jetties and groins while ignoring or even destroying coastal marshes despite their potential to provide protective benefit (Shepard et al., 2011). However, recent research has supported the importance of implementing natural infrastructure solutions also known as nature-based solutions as a means of adapting to climate change impacts (Sutton-Grier et al., 2015). These include but are not limited to living shorelines, managed realignment, and ecological restoration (Sutton-Grier et al., 2015). Natural infrastructure solutions can range from fully natural solutions to hybrid or more engineered solutions such as managed realignment or retention ponds (Bridges et al., 2015). The use of natural infrastructure approaches can increase resiliency and risk reduction, as the co-benefits that often accompany these approaches include ecosystem services such as erosion control and flood protection (Bridges et al., 2015). With managed realignment, tidal wetland restoration can lead to wave attenuation and sediment stabilization which leads to coastal storm protection. There are other benefits of ecosystem services such as water filtration, carbon and nutrient sequestration, and increased habitat for fish and other wildlife (Allen, 2000; Bridges et al., 2015).

There are generally three options for coastal management in relation to climate change adaptation: firstly, Reinforce i.e., "hold the line", Realign, for example managed realignment, and Relocate, e.g., managed retreat. There are other options such as Restriction which is a governance approach involving policy and regulation that restricts or limits coastal development, and Reimagining which involves thinking differently about coastal protection, this can also include the incorporation of nature-based or hybrid approaches to climate change adaptation strategies (Singh et al., 2007; Rahman et al., 2021 – in review).

Salt marshes are essential for coastal hazard mitigation and climate change adaptation (Shepard et al., 2011). There is need for the creation and implementation of policies that propose restoration or construction of natural systems that will maximize the benefits and ecosystem services of salt marshes (Shepard et al., 2011). Salt marshes are a practical choice for inclusion in mitigation and adaptation approaches as marshes occupy much of the same low-lying coastal areas that are especially vulnerable to sea level rise (Shepard et al., 2011). By means of accreting sediment at a level that is comparable or even higher than sea level rise, salt marshes are able to maintain the coastline, relative to sea level rise, providing a further reduction in vulnerability to hazards and climate change (Shepard et al., 2011).

Salt marshes can be used as foreshore protection to reduce the impact of storm surges and wind waves (Vuik et al., 2016). The wave heights that act on coastal dykes can be reduced by the application of vegetated foreshores (Vuik et al., 2016). Vegetation provides a barrier or supplies bottom friction that dissipates wave energy (Möller et al., 2002). However, there needs to be more research carried out regarding the efficiency of foreshores in reducing wave energy under severe storm conditions (Vuik et al., 2016). This thesis seeks to investigate the wave dissipation potential of salt marsh vegetation and investigate the effects of vegetation on decreasing the significant wave height under hypertidal conditions of the Bay of Fundy.

1.3. SALT MARSHES

1.3.1. Definition of salt marshes and their importance as a coastal ecosystem

Salt marshes are natural ecosystems that form in intertidal zones of coastal regions in mid- to high latitudes (Davidson-Arnott et al., 2019). These ecosystems exist where the energy levels are low enough to support the growth of mostly halophytic vegetation and sustain it even where frequently inundated (Allen, 2000; Friedrichs and Perry, 2001). Salt marshes have numerous benefits such as their ability to provide storage for nutrients, sediments, contaminants, and large amounts of carbon on a geological time scale (Allen, 2000; Leonardi et al., 2018). Salt marshes account for 46.9 % of the total carbon burial in ocean sediments (Duarte et al., 2013). They also have the ability to trap particles from the water flow, storing them in the soil (Duarte et al., 2013). Salt marshes also provide habitats for various animal species and protection from storm surges by acting as natural buffer zones, absorbing both wind and wave energy before it reaches inland (Allen, 2000; Foster-Martinez et al., 2018; Möller et al., 2014).

1.3.2. Salt marsh processes

In many areas around the world, salt marshes contribute to flood risk reduction by wave dissipation and provide protection against waves during storms as they act as a buffer (Möller, 2014). Salt marshes are important coastal ecosystems and are valued for their services such as their ability to sequester carbon, and their role in attenuating wave energy, which contributes to coastal resilience (Foster-Martinez et al., 2018); (Figure 1.1.) (Duarte et al., 2013).

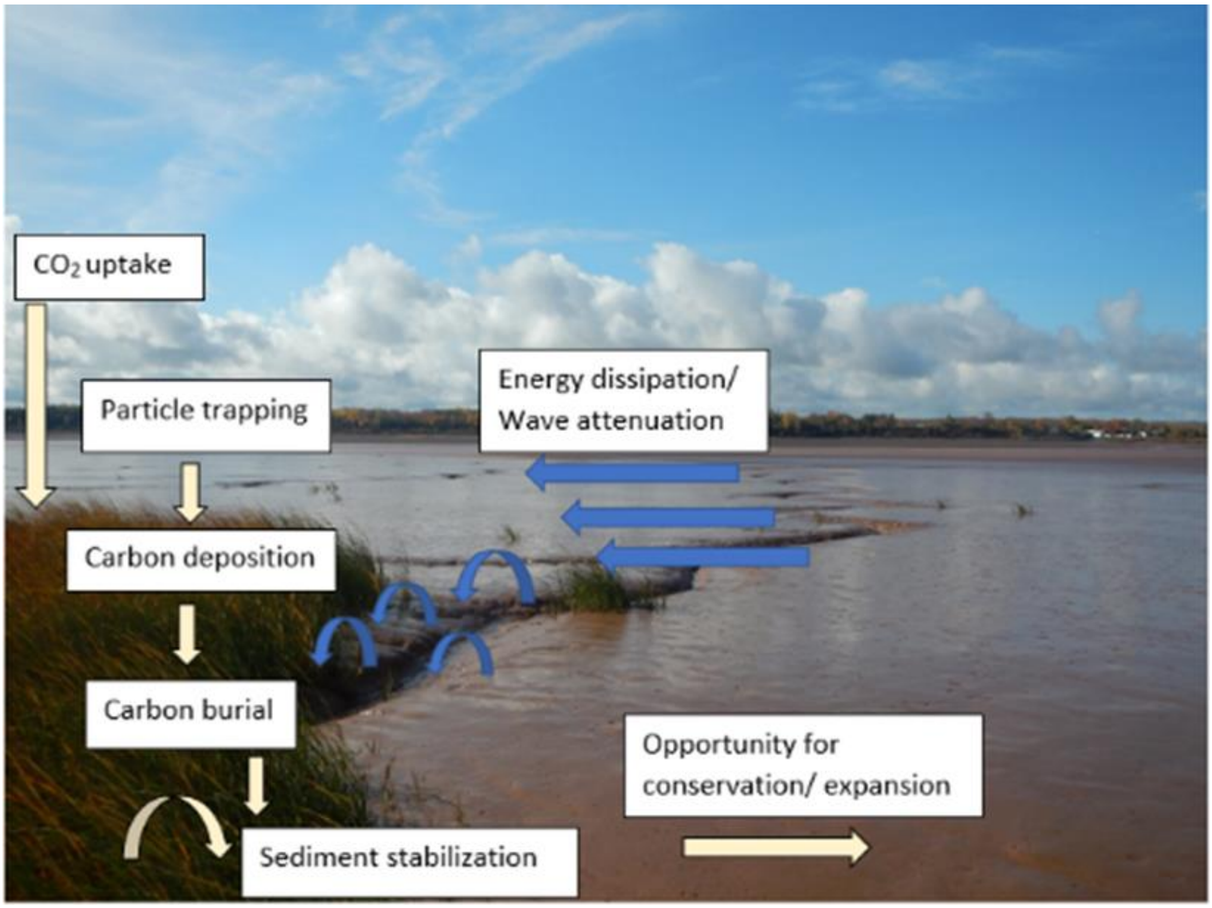

Figure 1.1. Salt marsh processes that affect their capacity for climate change mitigation and adaption. (modified From Figure 1. Duarte et al., 2013)

Salt marsh ecosystems are important for coastal defence as they have the ability to grow in the presence of sea level rise (Graham and Manning, 2007). As the sea level rises, it keeps pace with the accumulation of suspended particulate matter, if there is sufficient sediment available (Graham and Manning, 2007). Due to increasing rates of sea level rise, coastal marshes are reliant on a higher sediment supply, to vertically adapt to the rising sea level (Leonardi et al., 2018). The persistence of marshes depends on whether the surface accretion is higher than the rate of both subsidence and local sea level rise (Mitchell & Bilkovic, 2019). Feedbacks between tidal flooding, growth of plants and transportation of sediment allow for marshes to vertically adapt to a wide range of rising sea level rise rates (Kirwan et al., 2016). Flooding that is associated with RSLR promotes the growth of marsh vegetation which enhances mineral sediment settling and production of organic matter, allowing marshes to build elevation rapidly under faster rates of RSLR (Kirwan et al., 2016). However, in the lateral dimension, marsh edges are eroded by waves, leading to increased fetch and even greater erosion rates (Kirwan et al., 2016). Progradation occurs in low energy embayments (Kirwan et al., 2016) (See Figure 1.2. below).

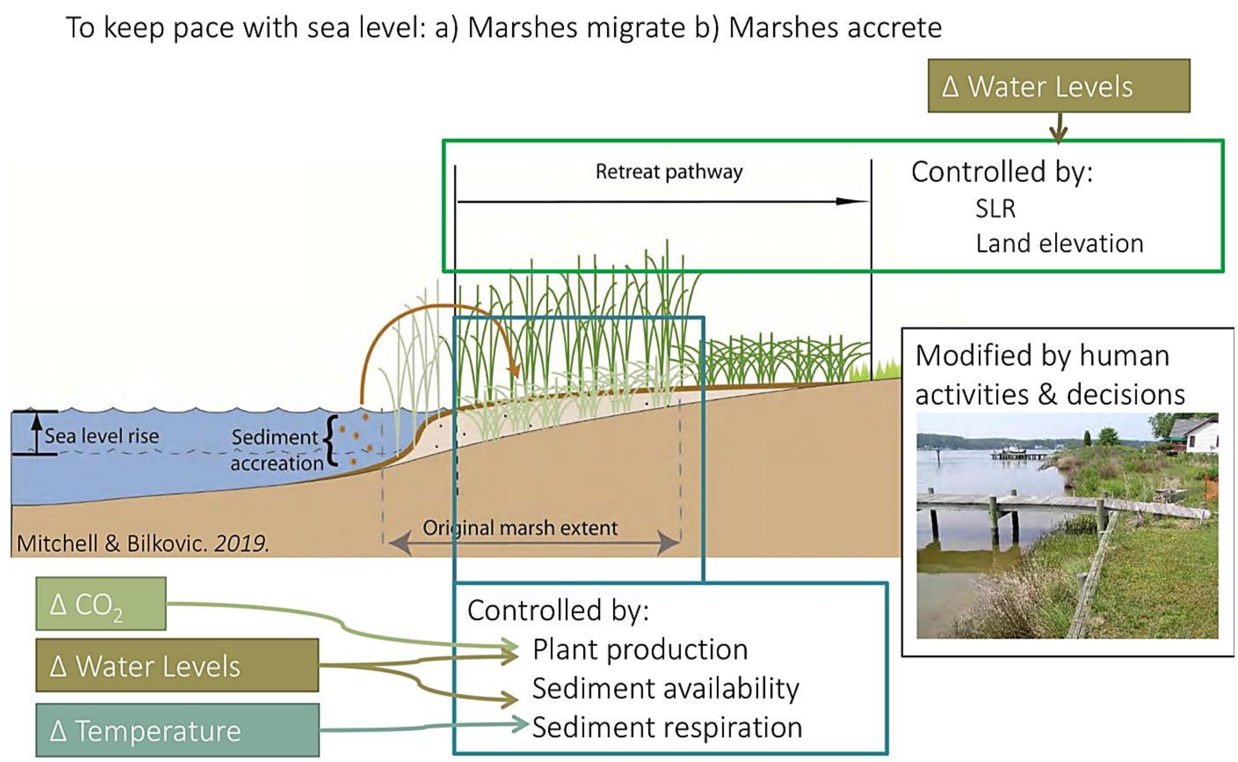

Figure 1.2. With rising sea level, foreshore marshes can adapt due the dynamic processes. The presence of tall dense marsh vegetation allows for wave energy dissipation and the collection of sediment which leads to an increase in marsh elevation; the roots of marsh vegetation also contribute to sediment accretion. Low elevation lands allow for the retreat of marshes into upland areas as sea level rises, maintaining marsh extent under changing conditions (Figure 1., modified from Mitchell & Bilkovic, 2019).

Salt marshes in macrotidal regimes are more resilient to high rates of sea level rise as well as reduced sediment supply, compared to salt marshes in microtidal regimes (Leonardi et al., 2018). Spatial variations in surface elevation and distance from tidal channels both control rates of sedimentation on natural marshes (Vandenbruwaene et. al, 2011). If a marsh platform is located much higher in the tidal frame, it is less likely to be inundated and the increase in elevation will be smaller (Vandenbruwaene et. al, 2011).

1.3.3. Characteristics of Salt Marshes

Occurring in mid- and high latitudes, and in some tropical areas, salt marshes contain salt-tolerant vegetation (Davidson-Arnott et al., 2019). Vegetation includes grasses, herbs, and small shrubs. Salt marshes consist of vegetated platforms that are gently sloping and three marsh zones - the high marsh, mid marsh, and low marsh zone (Davidson-Arnott et al., 2019). The low marsh zone is characterized by vegetation which can be submerged on almost every tide, for more than six hours (Davidson-Arnott et al., 2019). The low marsh is dominated by one or two species, due to the high stresses in this zone (Davidson-Arnott et al., 2019). Within the high marsh zone, there is a decrease in the frequency and depth and the vegetation may be submerged only briefly during spring high tides (Davidson-Arnott et al., 2019). The high marsh zone has an increased species abundance as a result of its more favorable conditions that allow for a wider range of plants (Davidson-Arnott et al., 2019).

1.3.4. Role of salt marshes in coastal protection

Salt marshes play an important role as natural defense systems against storm waves (Jadhav et al., 2013). Salt marshes provide humans with various ecosystem benefits, amongst which include their role as buffers that protect coastlines from waves during storms (Möller et al., 2014; Shepard et al., 2011).

There are many factors that can lead to a reduction in wave energy such as depth-induced wave-breaking, bottom friction or when energy is lost from surface waves that propagate through vegetation. All these factors lead to an overall decrease in wave height (Vuik et al., 2016). Wave dissipation is also dependent on the wave height to water depth ratio (Foster-Martinez et al., 2018). Seasonal variations in aboveground biomass and mechanical fragility also play a significant role in decreasing wave height (Vuik, 2016). In the summer, salt marshes are more effective at decreasing wave heights, compared to the winter where the vegetation coverage is minimal or where the vegetation is dead (Möller et al., 2014). Wave energy dissipation by vegetation is most effective when the water depth is low and where there is a high biomass (Vuik et al., 2016).

1.3.5. Salt marsh restoration and nature-based solutions

Approximately 25 – 67 % of intertidal wetland has been lost worldwide (Virgin et al., 2020). Within the Bay of Fundy, it is estimated that 85% of the estuaries have been lost due to agricultural dyking since the 17th century (Byers and Chmura, 2007). The loss of salt marshes can be attributed to changes in land use, coastal transformation, and reclamation (Duarte et al., 2013). Factors such as land use change, altered hydrodynamics and sediment supply; and the prevention of landward habitat migration by fixed sea defence lines, have led to areal losses of intertidal mudflats and salt marshes globally (Möller et al., 2002).

One way of encouraging salt marsh construction or re-development is through managed realignment, which is a common coastal management strategy for restoring completely tide-restricted marshes (Virgin et al., 2020). This promotes the development of salt marshes in front of a new dyke that is built inland (Virgin et al., 2020). Realignment involves allowing an area of previously reclaimed land to be re-inundated by the sea or tidal waters (French, 2006). If the land originally supported a salt marsh, then it has more potential to support such a development (French, 2006). Managed realignment or managed retreat is the shifting of the sea border landwards (French, 2006). There are immense benefits to the concept of allowing the development of salt marsh and intertidal mudflats, landward of existing ones through returning land to the sea (French, 2006). These include increased wave attenuation and a localised reduction in sea level rise impacts as a result of the increased tidal volume (French, 2006).

Salt marshes can also be restored or reactivated by creating a breach in the dyke (Byers and Chmura, 2007), or by removing a culvert (Bowron et al., 2011). In such a scenario, tides are reintroduced but there is no realignment, instead topography constrains the flooding waters. One of the important factors in salt marsh restoration is the hydrology which can alter the geomorphology of the site and (Bowron et al., 2011). When a dyke is breached by the sea or human intervention, salt marsh ecosystem functions may be restored passively, or actively (van Proosdij et al., 2010). Reintroducing seawater to a site aids in the re-establishment of processes that are essential for the survival of tidal marshes (Bowron et al., 2011). For restoration projects to be successful, there must be an understanding of both biotic and abiotic factors, and their interactions (Broome and Woodhouse, 1988). The return of seawater to the site is one of the key abiotic factors in salt marsh restoration (Zedler, 2000). This is because sediment dynamics, soil development, plant dispersal and growth and access for aquatic life is dependent on the hydrology (Zedler, 2000). Extensive monitoring is essential for salt marsh restoration activities, both pre- and post-restoration ((Zedler, 2000), this helps to ensure that appropriate measures were undertaken for the success of the project.

Marsh restoration and protection of natural marshes is important because large marshes with dense and productive vegetation can attenuate wave energy resulting in stable shorelines (Shepard et al, 2011). As a result of human use, sea level rise and increased storminess, coastal areas are experiencing immense pressure (Möller et al., 2014). This has promoted ecosystem-based approaches to reduce coastal storm risks and the use of natural and nature-based features to improve coastal resilience (Bridges et al., 2015). It is essential to protect already existing natural marshes, and where possible to create salt marshes, as they are a vital component of flood risk reduction (Bridges et al., 2015). Components of theses natural marshes play a vital role in wave energy dissipation, by means of attenuation (Bridges et al., 2015).

1.4. WAVE DISSIPATION

1.4.1. Waves

The significant wave height is the mean height of the highest one-third of all waves that are measured which is equivalent to the estimate that would be made by a visual observer at sea (Davidson-Arnott et al., 2019). The difference between the lowest point in the trough and the highest point in the following crest, is known as the wave height, H; while the wave period, T, is the time between the two downward crossing points (Davidson-Arnott et al., 2019).

Table 1. Wave Properties (From RBR Webinar - Tides and Waves (Siegel, 2020)

Wave Height (m)	**Wave Period (s)**
• Significant wave height (H_s, $H_{1/3}$, H_{mo})	• Significant wave period
• 1/10 wave height	• 1/10 wave period
• Maximum wave height	• Maximum wave period
• Average wave height	• Average wave period
Other Variables	
• Wave energy (J/m^2)	
• Tidal slope (m/hour)	

1.4.2. Definition of wave dissipation

Wave energy dissipation can be achieved by wave shoaling/breaking, removal of both plant and soil material from the marsh's edge, and by drag from the vegetation canopy (Möller et al., 2014). The presence of vegetation causes a significant amount of wave attenuation (Möller et al., 2014). Most wave energy dissipation occurs within the first few metres of the permanently vegetated salt marsh (Möller & Spencer, 2002). Vegetation plays a significant role in wave dissipation; an increase in vegetation density results in greater wave energy attenuated (Möller & Spencer, 2002). As waves reach vegetated shores, they lose energy due to obstructing vegetation (Jadhav et al., 2013). In turn, this reduces shore erosion and promotes shoreline protection (Jadhav et al., 2013).

When waves approach the coastal area, they first contact the sediment as the water becomes shallow (Koch et al., 2009). Waves may be attenuated depending on the fraction of the water column that the vegetation occupies (Koch et al., 2009). As the waves propagate through seagrass beds, they become less energetic as they approach the marsh (Koch et al., 2009). (Figure 1.3.)

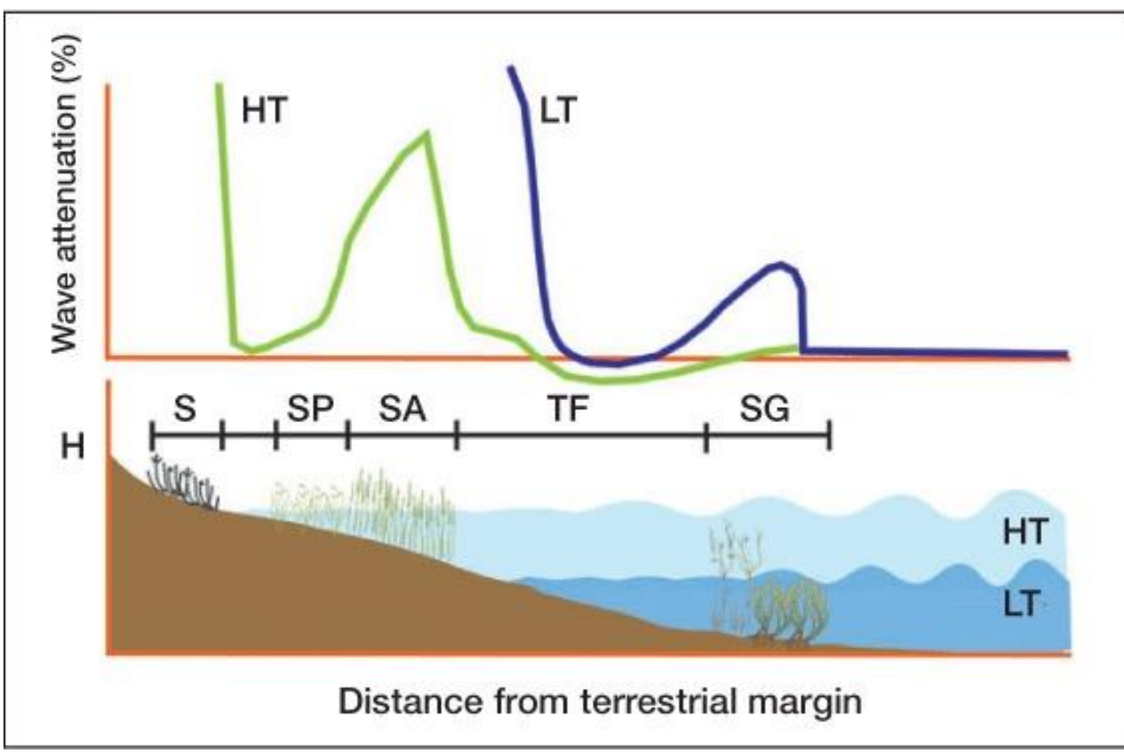

Figure 1.3. A schematic representation of the wave attenuation (%) at both high (HT) and low tide (LT) over a temperate coastal wetland. Other plants were included to show the cumulative effect they may have on wave attenuation, although they may not co-occur in nature.

SG: seagrass; TF: tidal flat; SA: Spartina alterniflora; SP: Spartina patens; S: Salicornia marsh. (Figure 4., Koch et al., 2009)

1.4.3. Factors that affect the wave dissipation potential of salt marshes

Climate change has an impact on wave heights and other wave parameters (Duarte et al., 2013). In the following sections, factors that affect wave dissipation of salt marshes will be discussed in detail.

1.4.3.1. Water depth

Wave attenuation depends on vegetation properties such as vegetation height, stem diameter, flexibility and spacing (Feagin et al., 2011). These properties affect the amount of wave force that vegetation can withstand (Feagin et al., 2011). Generally, dense and tall vegetation is highly effective for wave energy dissipation (Foster-Martinez et al. 2018). However, as wave height increases, stem breakage can occur, which limits wave dissipation factors (Foster-Martinez et al., 2018).

Some studies have shown that wave dissipation over submerged salt marsh canopies depends on water depth and incident wave energy and other hydrodynamic conditions (Möller et al., 2014). The relationship between submergence and total water depth (h); the relative wave height (H/h, where H is wave height), the width (b) of the field with respect to the incoming wavelength (L), which is the velocity divided by the frequency (Duarte et al., 2013). Longer waves require a wider domain to achieve damping (Duarte et al., 2013). The relationship between H and h is a ratio that closely controls wave breaking (Duarte et al., 2013). This ratio increases as waves are propagated towards the shore, due to the combined effect of wave shoaling and shallower depths (Duarte et al., 2013). When a threshold of 0.68 H for H/h has been reached, wave breaking occurs, hence, changes in bathymetry can contribute to dissipation (Duarte et al., 2013).

Strength of dissipation mechanisms depends on the wave height and water depth ratio (Feagin et al., 2011, Foster-Martinez et al., 2018). Lower water depths (i.e. shallow water) lead to greater wave attenuation, in cases where the vegetation is emergent (Rupprecht et al., 2015; Foster-Martinez et al., 2018). This has to do with the submergence ratio which is the ratio of water depth to canopy height. Vegetation dissipates waves better with decreasing submergence ratio (Rupprecht, 2017) as shown in Figure 1.4. below (Figure 4., Leonardi., 2018). A reduction in wave energy in shallow water is also due to various factors such as energy loss through viscous friction, percolation into the substrate and surface friction at the sea-bed boundary layer (Möller et al., 1999). Sediment trapping and settling occurs when the wave energy is lower, and this is vital for the existence of salt marshes (Foster-Martinez et al., 2018).

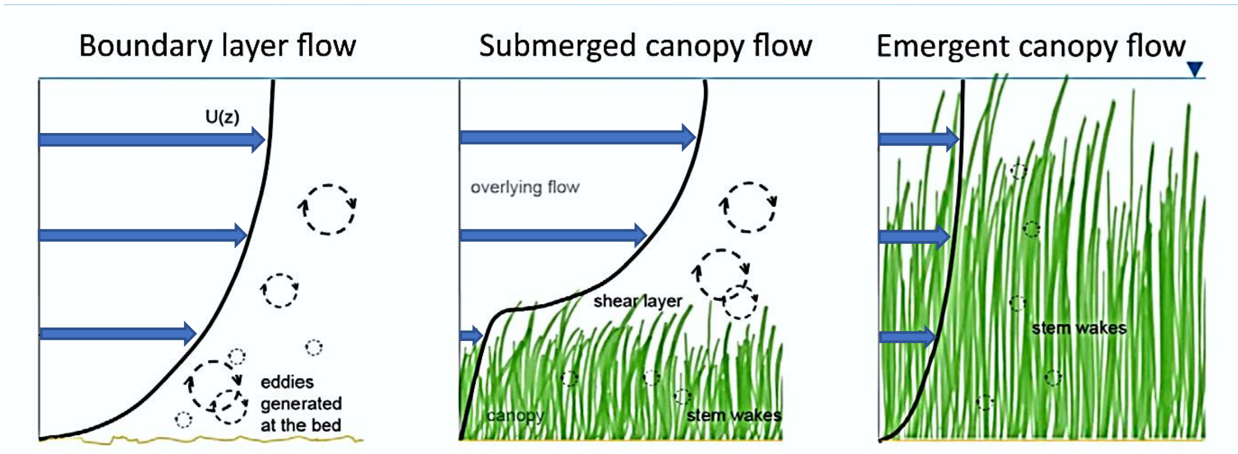

Figure 1.4. Different flow regimes shown with different flow profiles; no vegetation, submerged vegetation, and emergent vegetation, respectively. The presence of difference sources of turbulence within the flow is dependent on the vegetation height with respect to water depth. The dominant source of turbulence is the bed, the top of the canopy (sheer layer), and the stem wakes, respectively (from left to right). The blue arrows represent the flow and show the direction of the movement of water. (Modified from Figure 4., Leonardi et al., 2018) Canopies that are submerged reduce flow and turbulence (Duarte et al., 2013)

1.4.3.2. Bottom friction

Friction due to the presence of vegetation increases bottom roughness, reducing the near-bed flow velocity and elevating the bottom boundary layer (Duarte et al., 2013). A porous medium with a large energy dissipation capacity is provided by the stem density and flexibility (Duarte et al., 2013). Wave dissipation can occur through viscous friction, percolation into the substrate and surface friction at the sea-bed boundary layer (Möller et al., 1999).

1.4.3.3. Variations within salt marsh elevation, changes in frontal area vegetation

Coastal habitats that are vegetated have the capacity to provide coastal protection and can help mitigate impacts of sea-level rise and the associated increase in wave action (Duarte et al., 2013). Wave attenuation can be achieved by inducing wave breaking as the main damping mechanism, flow separation, and dissipation of energy through friction on rough surfaces (Duarte et al., 2013). The main dissipation mechanism is wave dissipation by vegetation (Vuik et al., 2016). There are various processes that lead to wave energy reduction (Vuik et al., 2016). Surface waves propagating through vegetation lose energy when they perform work on vegetation stems, branches, and leaves, resulting in a decrease in wave height (Vuik et al., 2016). When there is no vegetation present, waves can retain their energy further inland (Duarte et al., 2013). Wave attenuation by vegetation results in a gradual decrease in wave height and prevents the occurrence of intense wave breaking (Vuik et al., 2016). When vegetation is present, intense wave breaking is prevented since the wave energy is dissipated more gradually by the vegetation (Vuik et al., 2016). Wave breaking can lead to high sediment pick-up rates and severe erosion, hence the presence of vegetation is vital as it enhances the stable character of the salt marsh surface (Vuik et al., 2016).

Vegetation is an important factor that affects both the functioning and form of salt marsh ecosystems (Rupprecht et al., 2015). Other aspects related to vegetation that influence the wave dissipation potential include the vegetation density, the substrate's nature and quality, and the abundance of the aboveground biomass (Duarte et al., 2013; Möller and Spencer, 2002). Wave attenuation capacity is also influenced by the geometry of individual plants i.e. their roots, stems and canopies, the buoyancy, stiffness, and degrees of freedom (Duarte et al., 2013). Completely or partially submerged canopies reduce flow and turbulence, they increase the bottom shear stress and dampen wave energy and flow velocity (Duarte et al., 2013). This in turn promotes sedimentation which reduces sediment resuspension (Duarte et al., 2013).

The spatial configuration of vegetation patches and the ratio of water depth to canopy height affect plant-flow interactions, at vegetated landform scale (Rupprecht et al., 2015). However, at the scale of individual plants, mechanical aspects such as the flexibility of stems and buoyancy influence the magnitude of flow resistance provided and the drag force that is experienced by vegetation (Rupprecht et al., 2015). Under wave-generated orbital flow, the flexural rigidity is critical for plant behaviour and flow resistance (Rupprecht et al., 2015). Stems that are highly flexible tend to break and flatten for part of the wave cycle, with less flexible stems remaining upright (Leonardi et al., 2019; Rupprecht et al., 2015). This upright posture allows for the flow to travel through rather than over the canopy (Leornad et al., 2006; Rupprecht et al., 2015). The drag force is lower for canopies that are composed of flexible plants with low amounts of biomass, compared to stiff plants and large amounts of above ground biomass (Duarte et al., 2013; Rupprecht et al., 2015).

Vegetation contributes directly to the wave energy dissipation via plant-flow interactions, and indirectly through causing spatial variation in sediment accumulation, which in turn leads to the formation of topographic roughness (Rupprecht et al., 2015). Seasonal variations in aboveground biomass and mechanical fragility also influence the wave dissipation potential of salt marshes (Vuik et al., 2016). A significant degree of flow resistance might be achieved by basal stems and the branching of upper stems and their leaves (Rupprecht et al., 2015). Above ground biomass is a useful proxy for flexibility and buoyancy, as it varies with volume and density of plant material present (Rupprecht et al., 2015; Bouma et al., 2005). There has been an observed positive correlation between canopy density, above ground biomass and wave dissipation, at the scale of plant stands (Rupprecht et al., 2015). Non-stem components, specifically branches and leaves which constitute a significant proportion of the overall above ground biomass, can contribute significantly to wave dissipation (Rupprecht et al., 2015). Stem flexibility, biomass and vegetation density are key parameters that control the wave dissipation capacity of salt marshes, and hence their ability to establish and grow in coastal environments (Rupprecht et al., 2015).

Apart from vegetation properties such as vegetation height, stem density and spacing, wave attenuation also depends on hydraulic characteristics such as wave height, water depth and ambient currents (Vuik et al., 2016). Depth, wind speed or wind direction can limit the wave height (Vuik et al., 2016). At small water depths and with high biomass, wave energy dissipation by vegetation is most effective (Vuik et al., 2016). When the water depths are low enough, the wave-induced orbital flow can penetrate the canopy layer, and when the vegetation interacts with this flow an obstruction is formed (Rupprecht et al., 2015). This leads to the vegetation experiencing drag and re-orientation by wave forces (Rupprecht et al., 2015).

1.4.4. Summary of importance of salt marshes in wave dissipation

Wave attenuation over vegetated salt marshes can be significantly greater than over unvegetated intertidal surfaces (Möller et al., 2002). According to Möller et al. (2002), the most rapid reduction in wave heights occurs over the most seaward 10 metres of salt marsh vegetation. There is link between the cycle of vegetation growth and the average wave energy attenuation near the marsh edge (Möller et al., 2002). The presence of a vegetation cover results in additional friction, which in turn enhances dissipation over a salt marsh (Möller et al., 2002).

A combination of edge configuration and marsh surface roughness, allied to prevailing hydrodynamic conditions (including incident wave characteristics, direction of wave approach relative to the marsh edge and water depth) and their variability over time, affect the extent to which wave energy is dissipated (Möller et al., 2002).

Salt marshes are suitable for adaptive coastal management, as they can contribute to coastal protection (Willemsen et al., 2020). Salt marshes are a valuable component of coastal protection schemes (Möller et al., 2014). For natural features such as salt marshes to be included in quantitative flood risk assessments, further research on their capacity to act as wave dissipators under extreme level wave conditions should be carried out (Möller et al., 2014). This study provides a step towards closing the knowledge gap in coastal protection studies. Specifically, within the Bay of Fundy, there is need to gain a better understanding on the wave dissipation potential of salt marshes under extreme level wave conditions. This research will provide data which supports efforts towards building climate resilient communities and ecosystems through nature-based adaptation and implementation of natural infrastructure solutions (Virgin et al., 2020).

1.5. Summary of contribution of research to literature and implementation in coastal protection schemes

Salt marshes can be incorporated as a component of nature-based solutions to flooding. It is essential to test nature-based flood defences according to engineering standards for probability of failure, prior to considering them as full alternatives for conventional flood defences (Vuik et al., 2016). The probability that the flood defence fails in fulfilling its function is referred to as the probability of failure of a flood defence (Vuik et al., 2016). There is need for further research on the wave dissipation potential of salt marshes to gain a better understanding regarding coastal protection schemes (Vuik et al., 2016).

There needs to be a better understanding of vegetated intertidal environments and incoming waves, to achieve sustainable coastal management and planning (Möller et al., 2002). Marsh stability is an important aspect to consider in coastal flood risk reduction schemes (Möller et al., 2014). The presence of organic matter promotes resistance of the marsh surface to erosion by waves from above (Möller et al., 2014). Marsh surfaces can withstand larger wave forces without substantial erosion effects; this increases their reliability as a component of coastal defence schemes (Möller et al., 2014).

With more research and field studies on coastal protection, we can learn how to build climate resilient communities and ecosystems through nature-based adaptation and implementation of natural infrastructure solutions (Virgin et al., 2020).

1.6. Purpose and objectives

The purpose of this study is to determine the wave dissipation potential of salt marsh vegetation in a temperate, hypertidal estuary. The selected study site is Clifton Marsh, in the Upper Bay of Fundy, Nova Scotia. This site is important because it is monospecific, with *Spartina alterniflora*. This study will analyze the effectiveness of *Spartina alterniflora* on wave dissipation within a salt marsh, in the upper Bay of Fundy.

The research will address 2 key questions:

1. How effective is the *Spartina alterniflora* at attenuating wave energy over Neap/Spring tidal cycles?
2. How does *Spartina alterniflora*'s wave attenuation vary with varying heights of canopy and water depth?

CHAPTER TWO

STUDY AREA

2.1.The Bay of Fundy

The Bay of Fundy is located between Nova Scotia and New Brunswick (Desplanques & Mossman, 2004). It contains faults dating back to the Paleozoic era, which were activated during the opening of the Atlantic Ocean as a result of shifting plate tectonics (Desplanques & Mossman, 2004). This led to the creation of the Fundy basin by the sedimentary infill process (Desplanques & Mossman, 2004). The Bay of Fundy is characterised as a macrotidal estuary, experiencing a spring tidal range of 5.0 m at the mouth of the Bay, to over 16 m in the upper reaches (Byers and Chmura, 2004). The large tidal range is also a reason for the high suspended sediment concentration ranging from 0.2 to 30.4 mg L^{-1} as one moves up-bay, with an average of 6.6 mg L^{-1} (Amos and Alföldi 1979). Within the Minas Basin, in the main tidal basin, the concentration ranges from approximately 20 mg L^{-1} to 200 mg L^{-1}, but up to 70,000 mg L^{-1} in tidal rivers (Amos and Alföldi 1979).

The Bay of Fundy has unique tidal conditions which have led to the formation of expansive tidal wetlands that are minerogenic and macrotidal in nature (Byers and Chmura, 2014). Marshes build up with mineral matter, which is removed from the bottom, the banks, and the exposed shorelines of the Bay, due to the Bay of Fundy currents which have a high silt-carrying capacity (Desplanques & Mossman, 2004).

2.2.Clifton Marsh

Clifton Marsh is one of the Fundy type marshes which are built in a regime of tides with large amplitude and strong tidal currents (Desplanques & Mossman, 2004). Clifton marsh is a salt marsh at the confluence of the Shubenacadie and Salmon rivers in the Minas Basin in Nova Scotia (Figure 2.1.). Clifton Marsh is dominated by the salt-tolerant *Spartina alterniflora*, which largely depends on the delivery of sediment and minerals to the marsh via the tide. Marshes can self-adapt vertically and horizontally (Singh et al., 2007).

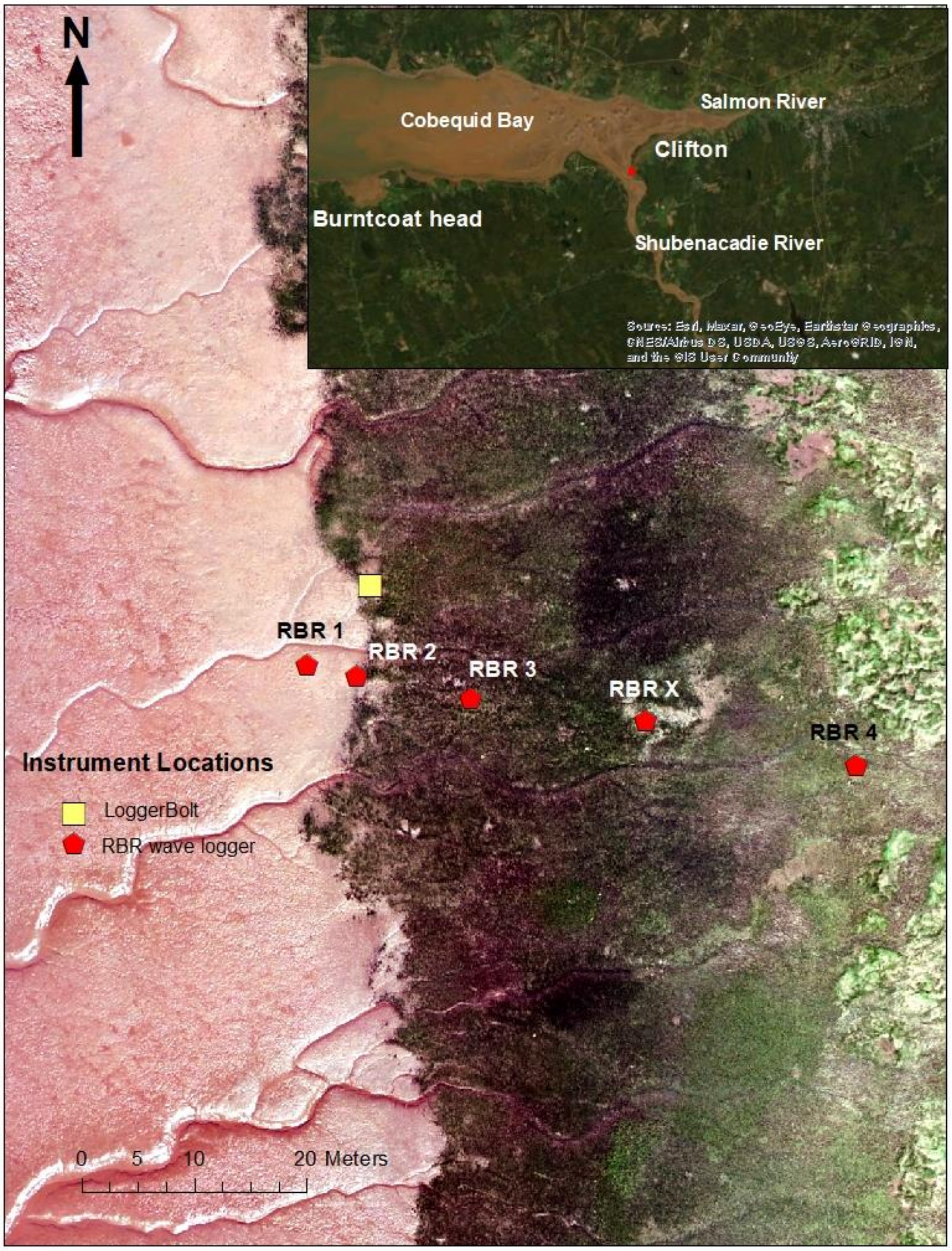

Figure 2.1. Study area map of Clifton Marsh, in the Upper Bay of Fundy, Nova Scotia.

Figure 2.2. Non-cliffed area, Clifton Marsh – Instruments deployed in a transect. (Imagery from June 27th, 2020, taken by Samantha Lewis at 120m above ground level, using DJI Phantom 4 RPAS. Direction of transect shown by red arrow)

Figure 2.3. Cliffed area, Clifton Marsh. (Oblique low altitude aerial imagery from June 27th, 2020, taken by Samantha Lewis). Aircraft altitude was 120m above ground level. Cliffs are located the South of the site.

CHAPTER THREE

METHODOLOGY

3.1.Field Methods

A transect was set up with 4 RBR*duet*³ T.D|wave16 — temperature and pressure loggers extending from the mudflat to the vegetated section dominated by *Spartina alterniflora*. Data were collected over a four-month period from mid-June to the first week of December 2020. Vegetation characteristics were measured at 2-week intervals throughout the growing season.

3.1.1. Wave measurement configuration

The instruments used for this experiment were the RBR*duet*³ T.D|wave16 — temperature & pressure (RBR Ltd, Canada).

The RBRs were set up in a transect, advancing from the unvegetated mudflat to the vegetated section of the marsh. Along the transect, the instruments were placed at 0, 5, 15, 25 and 50 m advancing into the vegetated marsh. One RBR was placed on the mudflat, directly in front of the marsh edge (RBR 1), the second RBR was placed at the edge of vegetation (RBR2). RBR 3, X and 4 placed in the vegetation, at 15, 25 and 50 m from the marsh edge (Vuik et al., 2016). RBR X was placed between RBR 3 and RBR 4, at the 25 m distance along the transect. This instrument was placed on the 19th of November 2020, upon realization that there was a much larger gap between RBR3 and RBR 4.

The RBRs were programmed to record the pressure with frequency of 4Hz over a period of 8.5 minutes, every 10 minutes. i.e., every burst contains 2048 samples (modified from Vuik et al., 2016). More information on the parameters recorded by these instruments is in the Appendix section, in Table A1. The pressure sensors were mounted exactly 0.10 m above the sediment surface (Vuik et al., 2016). Using an RTK-GPS device, the elevation at each station was determined and recorded relative to the Canadian Geodetic Vertical Datum 2013 (CGV2013) and the NAD83 CSRS UTM Zone 20 for the horizontal datum. The instruments were deployed between the 18th of June 2020 and the 3rd of December 2020. The aim was to capture full Neap to Spring cycle. Data were retrieved every two weeks to ensure smooth operation of the research.

Table 2: Coordinates of RBR instruments. Elevations at ground level in CGVD2013 datum.

Instrument	Distance (m)	Easting (m)	Northing (m)	Elevation (m)
RBR1	0	462285.10	5018938.00	6.148
RBR2	5	462289.50	5018937.00	6.250
RBR3	15	462299.60	5018935.00	6.501
RBRx	25	462315.06	5018932.57	6.976
RBR4	50	462333.80	5018929.00	7.168

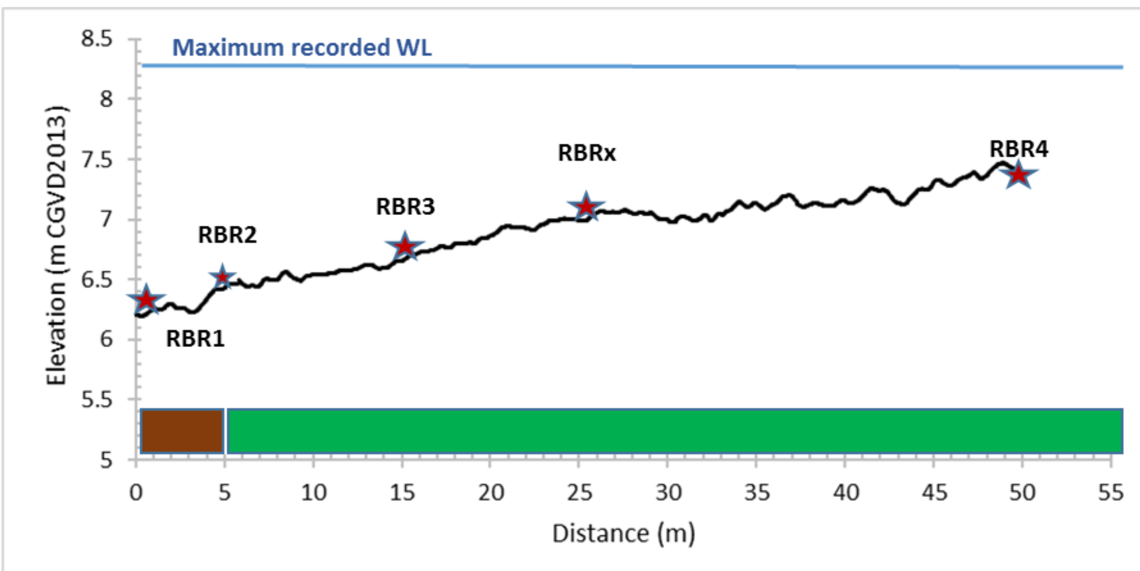

Figure 3.1. Cross sectional profile from DSM and RTK survey on June 29, 2020 indicating location of RBR instruments. Elevations relative to CGVD2013. Brown bar represents mudflat and green is Spartina alterniflora marsh.

3.1.2. Hydrology

A water level logger and a barometer logger were deployed at the marsh edge and on a tree, respectively. The loggers were deployed in on the 10th of August 2020 and retrieved on the 3rd of December 2020. A Hobo Barologger was attached to a tree proximal to the marsh, to record measurements which were used for compensating the data for atmospheric pressure. Using an RTK-GPS device, the elevation of the water level logger sensor at the marsh edge was determined and recorded relative to the Canadian Vertical Datum 2013 (CGV2013).

Figure 3.2. Location and set-up of Barologger on tree. Photo taken on August 17, 2020.

Figure 3.3. Location and set-up of Level logger at the marsh edge. Photo taken on August 17, 2020.

3.1.3. Vegetation measurements

Wave attenuation depends on vegetation properties such as vegetation height, stem diameter and spacing. Hydraulic factors such as wave height and water depth also play a significant role (Vuik et al., 2016). Vegetation surveys were carried out every two weeks on *Spartina alterniflora*.

Table 3: Summary of Clifton NS data collection, 2020.

Date	RBR 1	RBR 2	RBR 3	RBRx	RBR 4	Veg surveys
Wk. 1 (June 18 -24) Wk. 2 (June 25 - July 1)						✓
Wk. 3 (July 2 - 8) Wk. 4 (July 9 - 15)						✓
Wk. 5 (July 16 - 22) Wk. 6 (July 23 - 29)						✓
Wk. 7 (July 30 - Aug 5) Wk. 8 (Aug 6 - 12)						×
Wk. 9 (Aug 13 - 19)						
Wk. 10 (Aug 20 - 26)						✓
Wk. 11 (Aug 27 - Sept 2) Wk. 12 (Sept 3 - 9)						✓
Wk. 13 (Sept 10 - 16) Wk. 14 (Sept 17 -24)						✓
Wk. 15 (Sept 25 - 30) Wk. 16 (Oct 1 -7)						✓
Wk. 17 (Oct 8 - 14) Wk. 18 (Oct 15 -21)						✓
Wk. 19 (Oct 22 - 28) Wk. 20 (Oct 29 - Nov 4)						✓
Wk. 21 (Nov 5 - Nov 11) Wk. 22 (Nov 12 - Nov 18)						✓
Wk. 23 (Nov 19 - Nov 25) Wk. 24 (Nov 26 - Dec 3)						✓

Key
no data
data
no instruments on site

Data used for wave analysis

The vegetation characteristics near each station were analyzed. A 1 m x 1 m quadrat was used for vegetation surveys, with the subplot being 0.20 m x 0.20 m (20 cm x 20 cm) at each RBR station. Properties of all plants within the sub-plot were investigated between each station where the RBRs are deployed (Vuik et al., 2016). Individual stems were counted, the basal diameter and height of all individual stems was measured. Individual leaves were also counted, and the middle and top width of leaves was measured. Callipers were used for all leaf width and basal diameter measurements and a metre ruler was used to measure the stem height.

Near bottom density, stem density, mean stem height and maximum height will also be measured. Other values will be derived by calculation such as the estimate total biomass (Estimate total biomass *M* was estimated by multiplication of h_{mean}, $N_{v,0}$ (which is average stem height) and the near-bottom surface area $A_{v,0} = \pi b^2_{v,0}/4$ (Vuik et al., 2016).

Figure 3.4. Vegetation measurements of Spartina alterniflora, within flagged plots. Photo taken on July 30, 2020.

3.1.4. Aboveground biomass

Vegetation at each station was excavated within metal frame, with a 15 cm diameter, for aboveground biomass calculations. Vegetation samples were collected on the 5th and 19th of November 2020 and the 3rd of December 2020, as these were the selected days to harvest for aboveground biomass. The plants were clipped at the base of the stem and packaged in a very large plastic bag to avoid crushing of the plants. The excavated vegetation was transported in a cooler and refrigerated prior to being analysed in the laboratory.

3.2.Laboratory Processing

1.6.1. Vertical biomass distribution

Upon analysis, the shoots were separated, and the shoot density was measured. Sediment was rinsed off from the vegetation. The biomass sample was divided into living and dead vegetation, and the length of the vegetation was measured (Neumeier, 2005). Using a plastic kitchen board, a 5.0 cm interval was used to measure the designated canopy layers. The plants were placed in an approximate natural position on the kitchen board, and cut into segments of 5.0 cm, corresponding to horizontal layers of the canopy. All fragments of a given layer were placed into a small, pre-weighed aluminium tray, and dried at 80 °C for 48 hours, and then re-weighed (Neumeier, 2005). The biomass layer was obtained by subtracting the dish weight from the dish + sample weight. To obtain the total dry weight biomass, all the layers were added. All measurements were then divided by the area enclosed by the metal frame to obtain units per square metre (Neumeier, 2005). The results are weights per layer per ground unit (kg layer $^{-1}$ m^{-2}). The results can be presented as a percentage of total biomass per layer in order to compare relative distribution of different canopies (Neumeier, 2005).

1.6.2. Wave data analysis

The Ruskin RBR software generated the wave statistics which were used for the analysis. The wave data was exported analysed using Microsoft Excel. For each two-week dataset, the data was sorted to include only that with a depth greater than 0.1 m because the sensor was mounted 0.1 m above the bed which means that anything below 0.1 m was an indication that there was no water covering the instrument. Using the filter function in the Data tab, the filter was created to include data with a depth greater than 0.1 m. Following the creation of this filter, the events in the tides tab were selected to have a significant wave height that is greater than 0.05 m, for each deployment.

CHAPTER FOUR

RESULTS

4.1. Vegetation Data

Vegetation surveys were carried out bi-weekly and the parameters measured include stem height, stem density, basal diameter, middle and top leaf widths. The graphs below show the results from the three different vegetation stations, RBR2, RBR3 and RBR4, from June 18 to December 3, 2020. All graphs reflect a change in vegetation growth throughout the deployment season, with focus on the specific parameters measured.

The overall trend is a steady increase in stem height and basal stem diameter from June 18, 2020 to July 30, 2020. Figure 4.1a shows the average stem height for the duration of the deployment. There is an increase in average stem height from June 18, 2020 to August 27, 2020. Figure A1 in the Appendix section is a box and whisker plot which shows the stem height values that were recorded from June 18 to December 3, 2020. RBR 3 has greater values for stem height, represented by the box and whisker plot. RBR 3 also has the greatest mean stem height value of 61.5 cm. The rest of the mean values are 46.0 cm and 54.2 cm for RBR 2 and RBR 4, respectively.

The highest average stem heights recorded were 78.0 cm at RBR 2, 76.2 cm at RBR 3 and 63.5 cm at RBR 4 on August 27, September 10, and September 24, respectively. The highest average stem basal diameter values recorded were 7.82 mm at RBR 2, 9.30 mm at RBR3 and 5.66 mm at RBR 4 on July 30, and August 17, respectively.

According to Figure 4.1b there is a steady decrease in average stem diameter from August 27 to December 3, 2020. The stem diameter values recorded on August 27 are 5.40 mm, 4.74 mm, and 5.04 mm at RBR 2, RBR3 and RBR 4, respectively. The stem diameter values recorded on December 3 are 3.93 mm, 3.62 mm, and 3.03 mm at RBR 2, RBR3 and RBR 4, respectively. The average stem diameter decreased by 1.47 mm, 1.12 mm, and 1.11 mm, at RBR 2, RBR3 and RBR 4, respectively.

Figure 4.2 shows the changes in stem density throughout the deployment period. The highest increase in stem density occurred between August 17 and October 22, 2020. The stem densities recorded on August 17 were 475.00 stems/m^2, 500.00 stems/m^2 and 325.00 stems/m^2 at

RBR 2, RBR 3 and RBR 4, respectively. The stem densities recorded on October 22 were 1000.00 stems/m^2, 550.00 stems/m^2 and 325.00 stems/m^2 at RBR 2, RBR 3 and RBR 4, respectively. The highest stem densities were 2625.00 stems/m^2, 1875.00 stems/m^2 and 1000.00 stems/m^2, and were recorded on October 8, 2020, for RBR 2, RBR 3 and RBR 4, respectively. From these values, there is clear decrease in stem densities from the edge of the marsh (RBR2), to RBR 3 and lastly RBR 4.

Figure 4.3 shows the changes in middle and top leaf widths from June 18 to December 3, 2020. There is a sharp increase in both middle and top leaf widths from June 18 to July 16, 2020. The middle leaf width recorded at RBR 2, RBR3 and RBR 4 increased from 6.63 mm to 8.71mm, 7.32 mm to 8.21 mm and 6.97 mm to 7.91 mm, respectively, between June 18 and July 16, 2020. The top leaf width recorded at RBR 2, RBR3 and RBR 4 increased from 2.42 mm to 3.49 mm, 1.80 mm to 3.34 mm and 2.05 mm to 3.06 mm, respectively, between June 18 and July 16, 2020. The general trend at RBR 2, RBR 3 and RBR 4, is a steady decrease in the middle and top widths. The middle leaf widths decreased from 7.31 mm to 3.93 mm, 7.23 mm to 4.55 mm and 5.92 mm to 3.24 mm, respectively, while the top leaf widths decreased from 2.84 mm to 1.70 mm, 2.72 mm to 1.87 mm and an increase from 1.84 mm to 2.16 mm between August 20 and December 3, 2020.

Figure A3 in the Appendix section shows the differences in the aboveground biomass distributions. According to Figure A3, the calculations show that RBR 3 had the greatest aboveground biomass, followed by RBR 2, then RBR 4. The aboveground biomass values help us to see the changes in vegetation above the ground towards the last few weeks of the deployment.

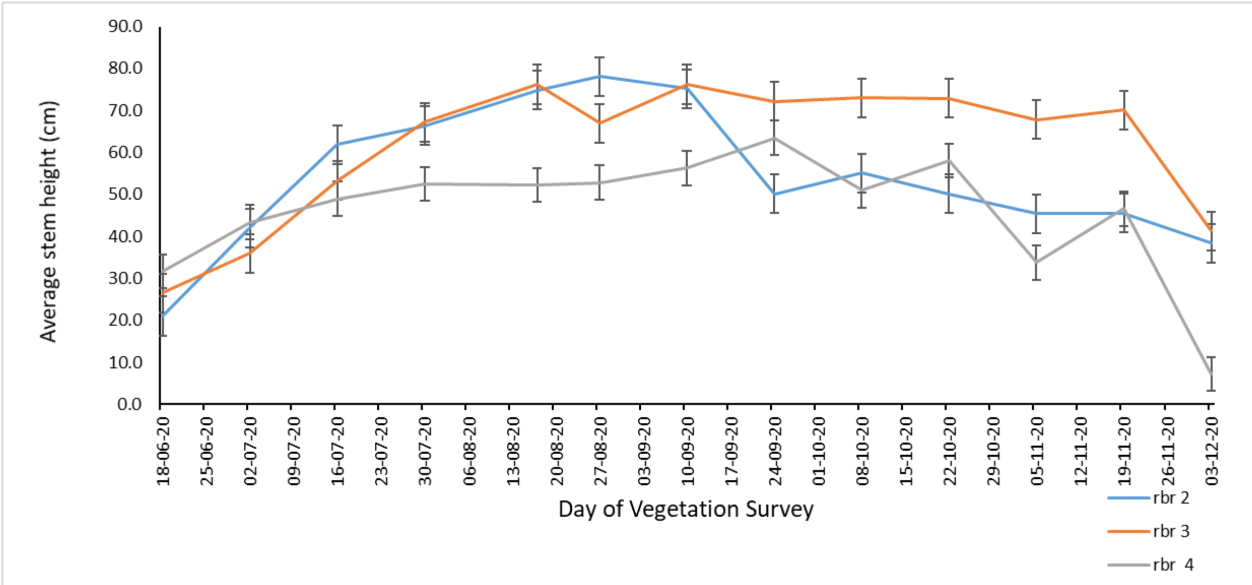

Figure 4.1a. Changes in average stem height of Spartina alterniflora from June 18 to December 3, 2020.

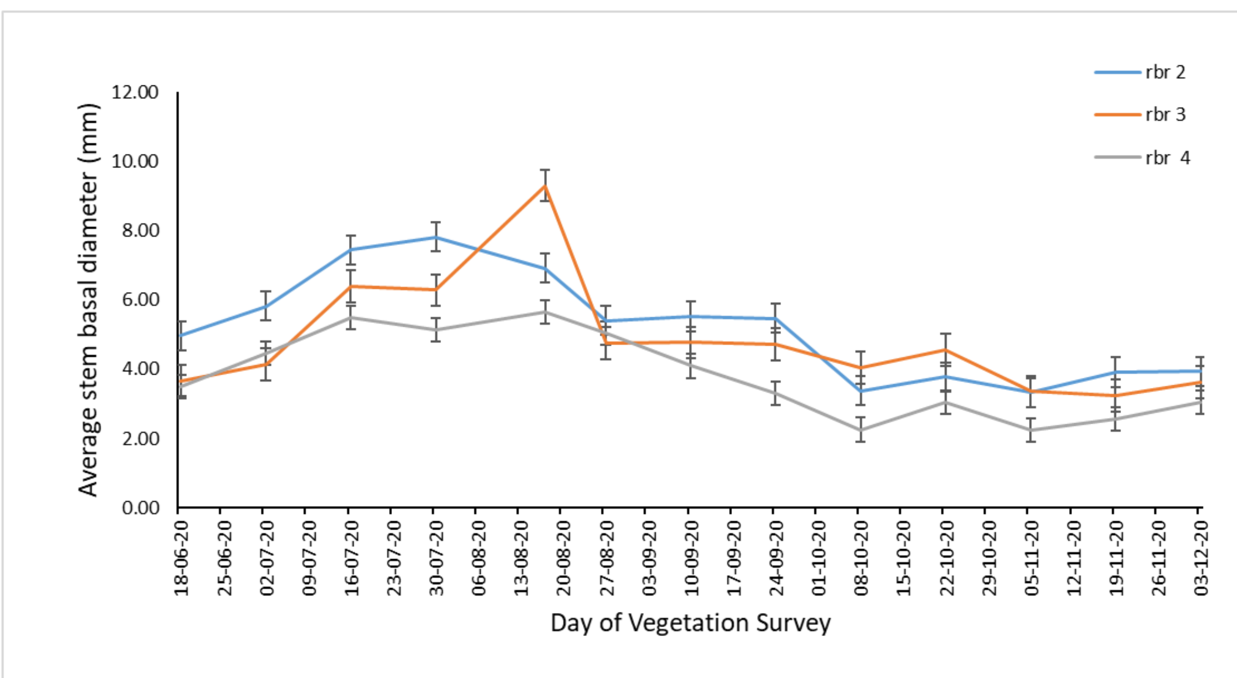

Figure 4.1b. Changes in average stem basal diameter of Spartina alterniflora from June 18 to December 3, 2020.

	RBR 1	RBR 2	RBR 3	RBR 4
Mean height (cm)	0	54.2	61.5	46.0
Mean basal diameter (mm)	0	5.20	4.8	3.83

Figure 4.1c. Changes in average stem height of Spartina alterniflora from June 18 to December 3, 2020. Overall mean height from all of these data at each station as well as basal diameter are provided.

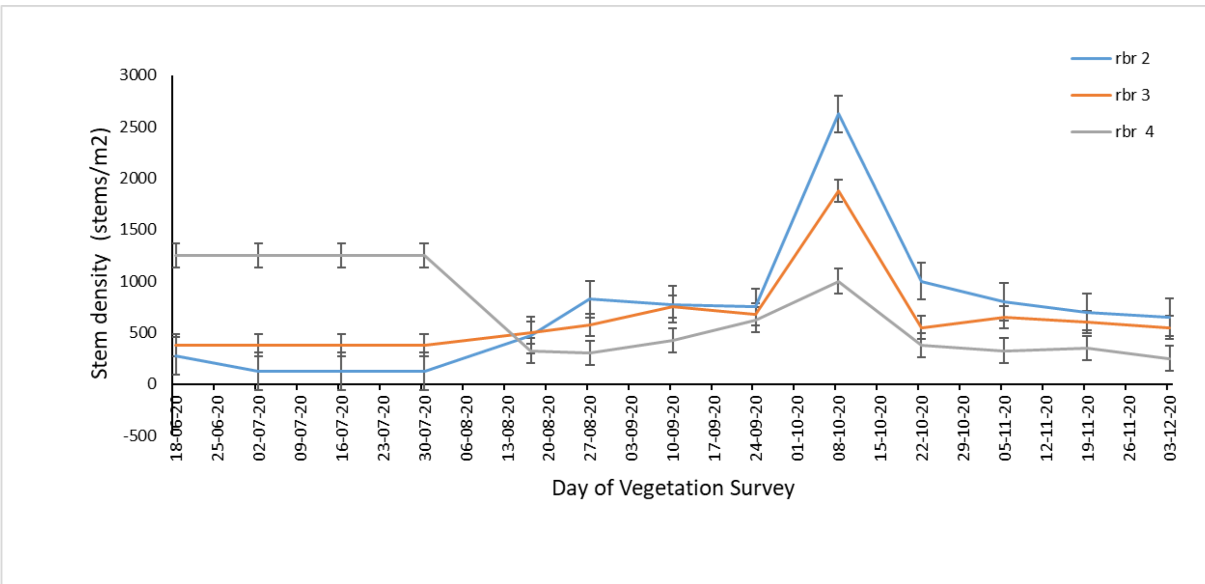

Figure 4.2. Changes in average stem density of Spartina alterniflora from June 18 to December 3, 2020.

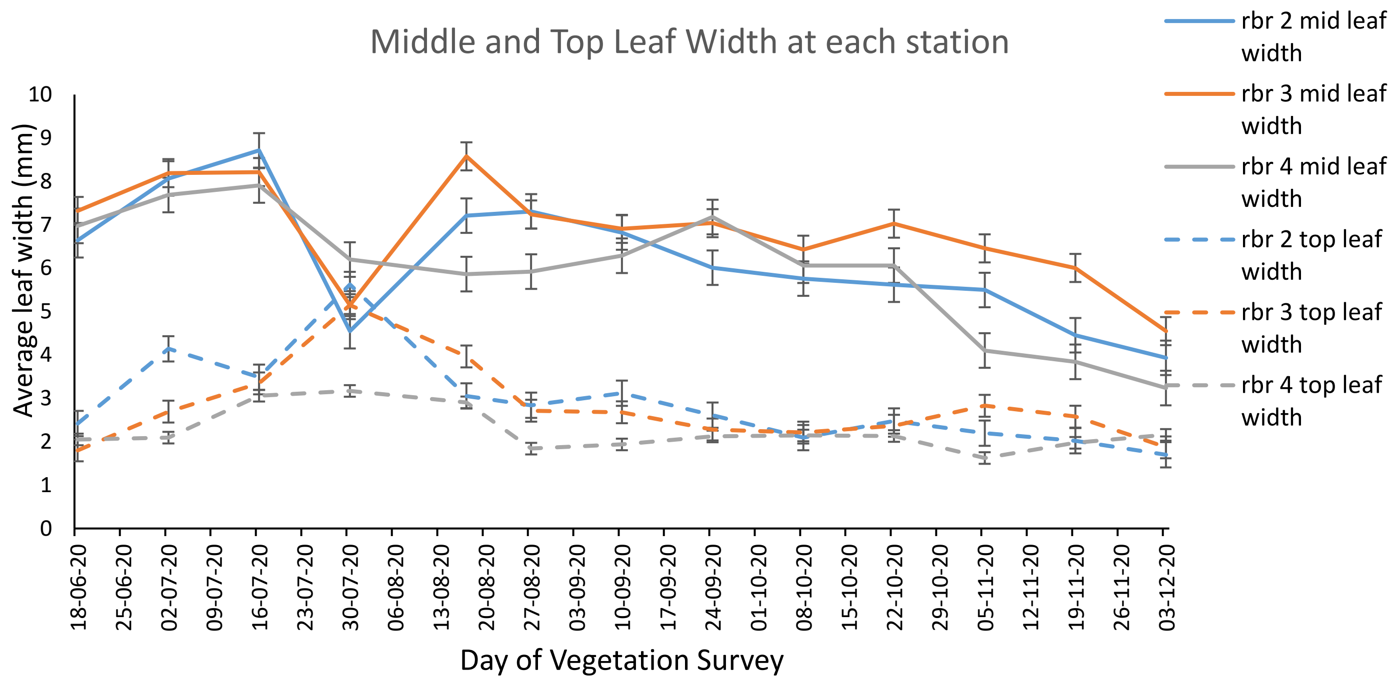

Figure 4.3. Changes in average leaf widths of Spartina alterniflora from June 18 to December 3, 2020.

4.2. Waves and Water Levels

The data recorded by the RBR*duet*³ T.D|wave16 — temperature and pressure loggers which were deployed in a transect at Clifton Marsh were analysed using MS Excel. The data were exported from the Ruskin software and only data from August 20 to December 3, 2020 were used for the analysis, because that particular time frame contained complete datasets for all instruments. There was a total of 53 tides recorded which were used for the analysis, with a sampling rate of 4 Hz and a sampling interval of 10 minutes. Each 10 minutes recorded 2048 data points, leading to 8.5-minute bursts every 10 minutes. Wave periods of 2.04 to 512 seconds were captured using these settings.

This section will begin with an analysis of the wave data, which were recorded from August 20 to December 3, 2020, analysing how the wave attenuation varies with varying heights of the canopy and water depth, and will conclude with a look at how relative roughness (RR) affects the significant wave height and the wave energy.

Figure 4.4 shows a frequency distribution of wave height classes that were used for the analysis based on the significant wave height recorded at RBR 1 at high tide. The data were sorted with a filter of depth which is greater than 0.10 m and the significant wave heights were sorted to be greater than or equal to 0.05 m. According to Figure 12, the 5 – 10 cm, 10 – 20 cm, 20 – 30 cm and > 30 cm wave height class contained 21, 21, 7 and 4 tides, respectively. The 5 – 10 cm and 10 – 20 cm wave height classes both had the highest number of tides, 21, while the > 30 cm wave height class had the least number of tides, 4.

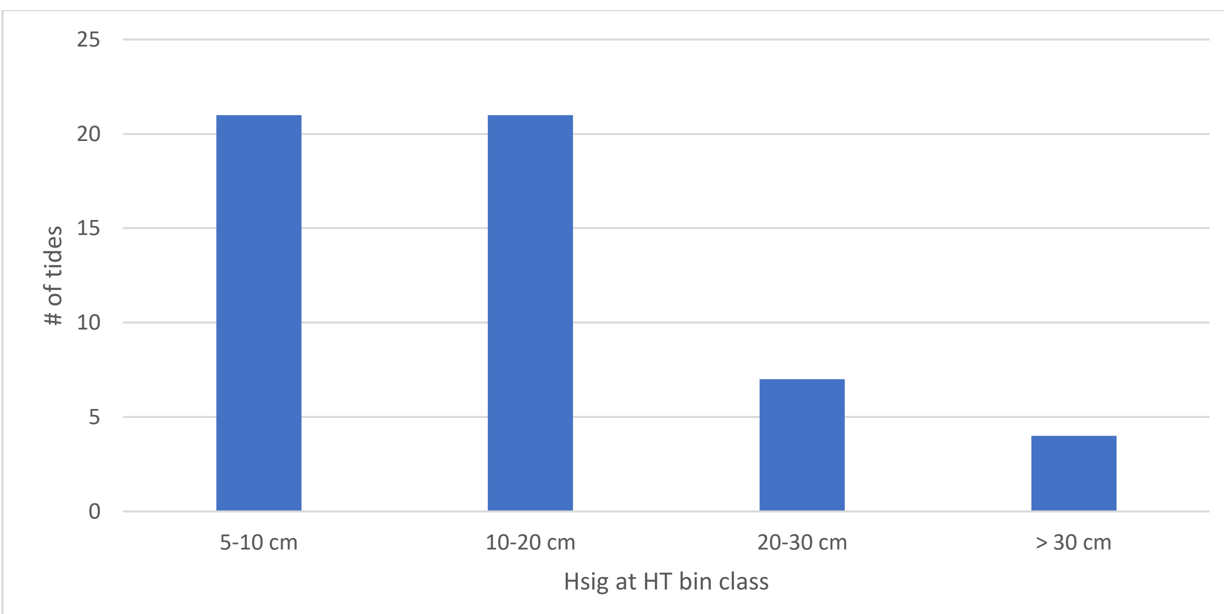

Figure 4.4. Frequency distribution of wave height classes used for analysis based on significant wave height recorded at RBR1 at high tide.

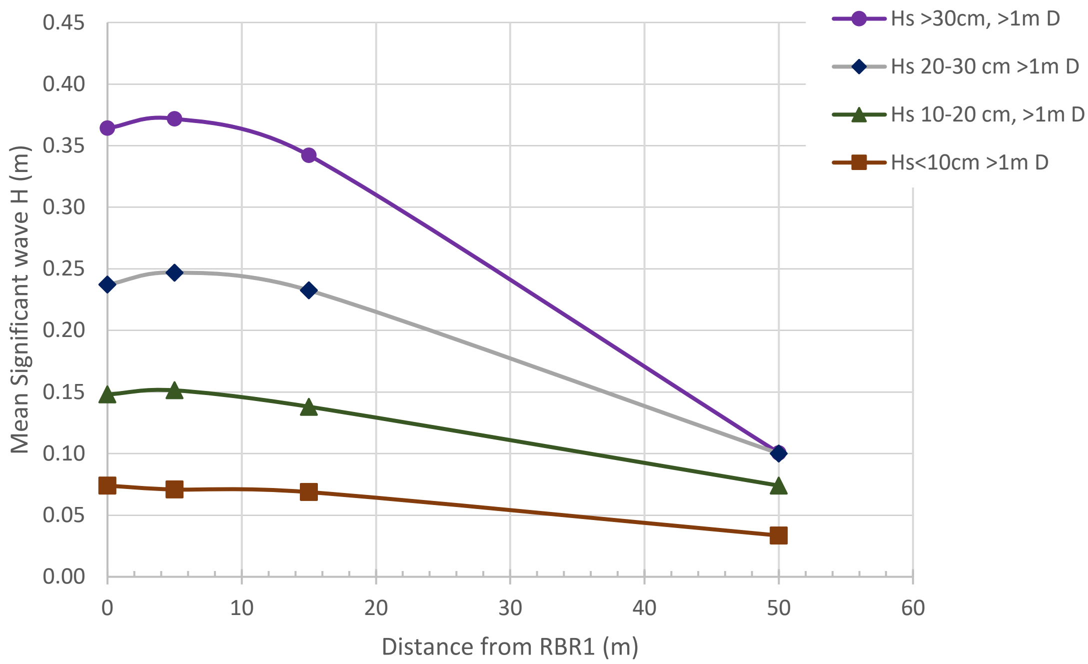

a)

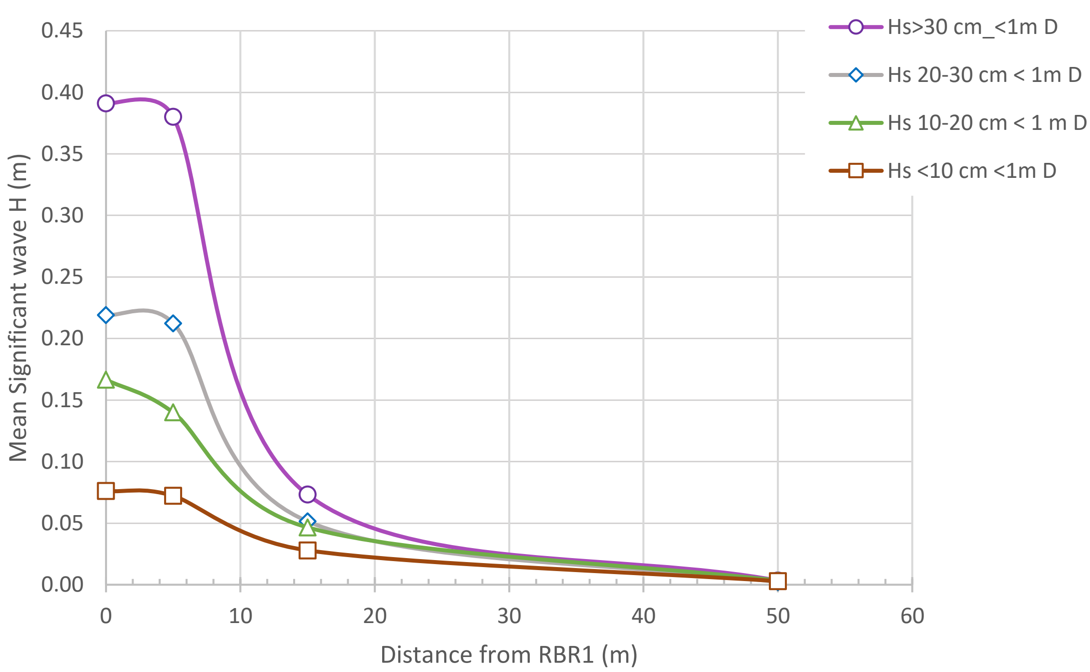

b)

Figure 4.5. Change in mean significant wave height at high tide from RBR1 to RBR4 50 m into the marsh for tides with a) high tide (HT) water depth greater than 1 m and b) HT less than 1 m.

The above figures show the changes in mean significant wave height (H_s) at high tide from RBR1 to RBR4 50 m into the marsh. Figure 4.5a and Figure 4.5b show these mean significant height values at HT, water depth greater than 1 m and water depth less than 1 m, respectively. There is an evident difference between the waves with a water depth less than 1 m, and those with a water depth greater than 1 m. Figure 4.5a shows the mean significant wave height values where the water depth is greater than 1 m. There is an initial increase in mean significant wave height which is proportional to the height to the wave, from RBR 1 to RBR 2. This could be a result of a bigger wave which comes into the shore and touches the bottom resulting in an increase in height as the wave is shoaling. Figure 4.5a shows a decrease in slope within the first 10 m of the canopy - the slope between RBR 2 and RBR 3 starts to decrease due to the presence of vegetation. The rate of decrease between RBR 2 and RBR 3 is a much greater rate of decrease in the larger waves.

However, this relationship is different where the water depth is less than 1 m. Figure 4.5b shows the mean significant wave height values where the water depth is less than 1 m. For lower water depths, the waves are attenuated to some extent over the mudflat surface. In this case, the decrease in mean significant between RBR 2 to RBR 3, for water depths less than 1 m, occurs over a much shorter distance. We see convergence almost to a very similar height within 10 metres of the vegetated platform, and a complete dissipation by 50 m.

Table 4: Summary of wave characteristics at each RBR station from Aug 18 to Dec. 3, 2020 based on output from RBR Ltd. Software, Ruskin.

	Decrease in Significant Wave H (%) relative to RBR1			
WD > 1 m	**N (# tides)**	**Distance from RBR1 on mudflat (m)**		
Hsig class		**5**	**15**	**50**
< 10 cm	13	4.2	7.1	54.9
10-20 cm	13	-2.3	6.8	50.1
20-30 cm	4	-4.1	2.0	57.8
> 30 cm	1	-2.1	6.0	72.4
WD < 1 m	**N (# tides)**	**Distance from RBR1 on mudflat (m)**		
Hsig class		**5**	**15**	**50**
< 10 cm	8	5.2	63.4	100
10-20 cm	8	16	72.0	100
20-30 cm	3	3.1	76.5	100
> 30 cm	3	2.8	81.3	100

Upon having placed the tides in different significant wave height classes, the percent decrease in significant wave height relative to RBR 1 was calculated. Table 4 is a summary of wave characteristics at each RBR station from Aug 18 to Dec. 3, 2020 based on output from RBR Ltd. Software, Ruskin. There is a clear difference in the capacity of vegetation to attenuate wave heights during spring versus neap tides and difference between Hsig classes. The greatest percentage decrease in significant wave height was 100%, at RBR 4, for all Hsig classes, where water depths are less than 1 m. The least percentage decrease in significant wave height was -4.1%, at RBR 2, for the 20 – 30 cm Hsig class, where water depth is greater than 1 m. The -4.1 % reflects an increase in significant wave height which is due to the impact of shoaling waves. Figure 4.5b shows a decrease in significant wave height of over 50 % at 50 m, whereas Figure 13b shows a decrease in significant wave height of over 60 % within the first 10 m. At the 50 m, complete wave attenuation would have occurred at RBR4, shown by a 0 value for mean significant wave height as shown in Figure 4.5b.

For water depths at high tide greater than 1 m, the frictional effects of bare mudflat were only recorded for waves less than 10 cm, all others saw increased wave heights likely associated with shoaling waves (Figure 4.5a). Wave attenuation was less than 10%, 10 m into the vegetated surface (Figure 4.5a). However, by 50 m within the vegetated canopy, when the maximum water depth was within the canopy (mean RR 1.16), between 50 to 72% of wave height was reduced. The decrease was most pronounced for larger wave conditions (Figure 4.5a). However due to the low number of tides from which this analysis was derived, Table 4 should be interpreted with caution.

For tides with water depths at high tide less than 1 m the attenuation capacity of the vegetation was evident. In addition, under all wave conditions for these tides, the frictional effects of the mudflat surface reduced wave heights between 3.1 % for waves 20-30 cm to 16 % for 10-20 cm waves (Table 4; Figure 4.5b). The 10-20 cm wave class saw a 16 % decrease in wave heights. 63.4 – 81.3 % of wave height was attenuated within the first 10 m of vegetated foreshore (Table 4; Figure 4.5b). During this measurement period, the vegetation occupied all the water column with RR of 1.32 and 2.24 at RBR2 and RBR3 respectively. There is a 100 % decrease in significant wave height at RBR 4, which can be explained by the complete submergence of vegetation within the water column. The RR at RBR4 was 3.92, the mean stem height at RBR 4 was 43.0 m, with a mean basal stem diameter of 3.83 mm. Wave heights were almost completely reduced 50 m into the vegetated surface.

4.3. Wave Data vs Vegetation Data

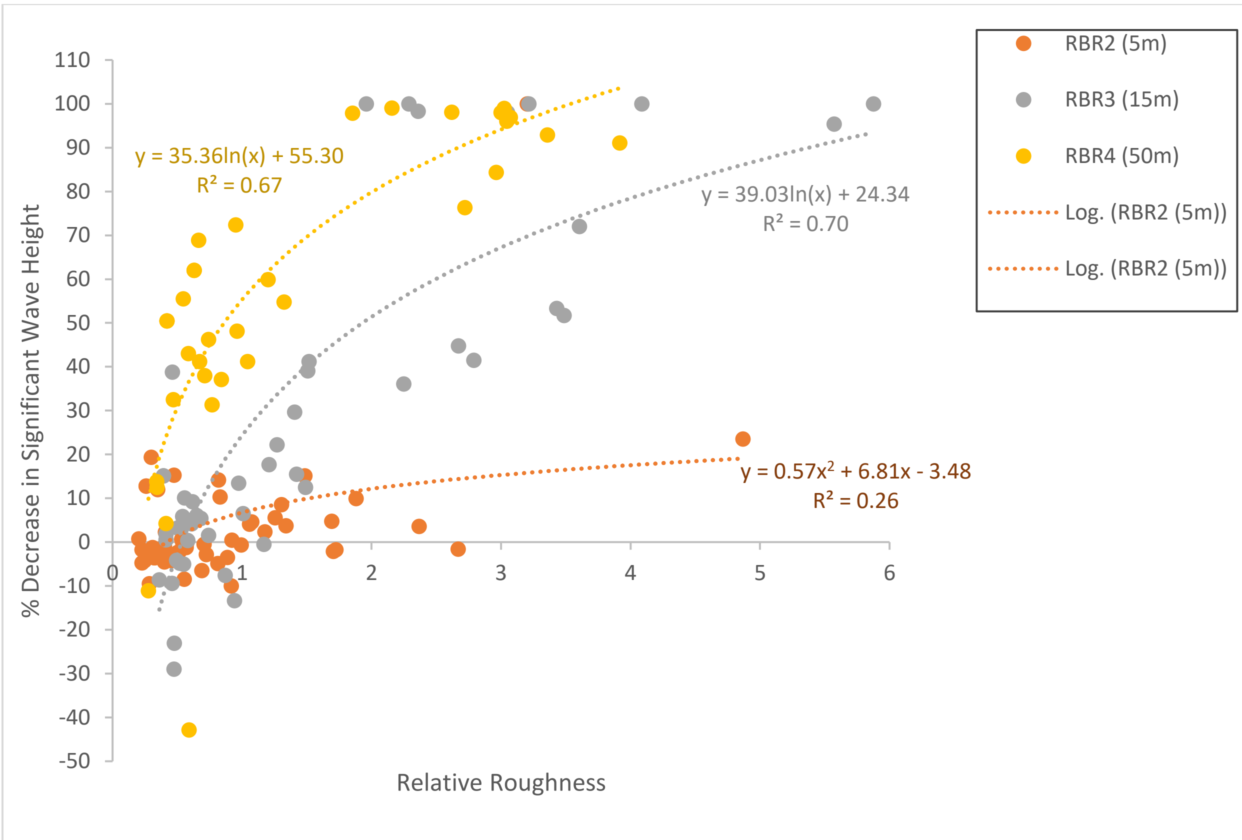

Figure 4.6. % Decrease in significant wave height versus RR (veg h/water depth)

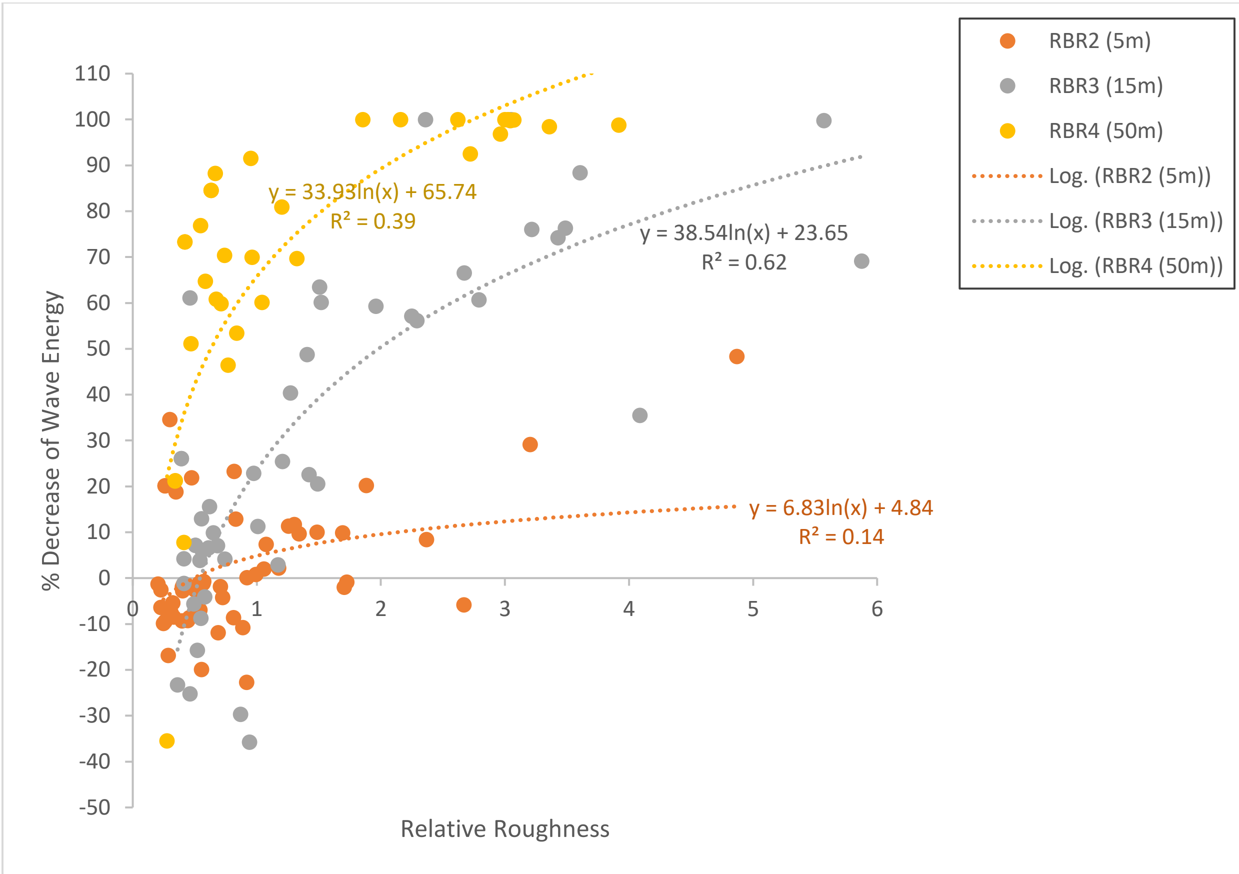

Figure 4.7. % Decrease in Wave energy versus RR

Figures 4.6 and 4.7 show the decrease in significant wave height and wave energy, all versus relative roughness, respectively. The general trend that is observed is the decrease in both significant wave height and wave energy is greater as you advance from the mudflat to the vegetated section of the transect. For the decrease in significant wave height, the R^2 values are 0.26, 0.74 and 0.67, for RBR 2, RBR3 and RBR 4, respectively. For the decrease in wave energy, the R^2 values are 0.30, 0.65 and 0.39, for RBR 2, RBR3 and RBR 4, respectively.

Relative roughness (RR) is a measure of the relative amount of the water column at a given time that is physically occupied by vegetation. It does not consider the energy dampening effects of the moving vegetation canopy. An RR value of 1.0 means that the vegetation canopy occupies the entire water column. With the large tidal range of the Bay of Fundy, *Spartina* marshes will therefore at a period in the tide have a RR of 1.0 but at high tide, particularly with superimposed wind waves, this value will be far less.

At RBR 3, the R^2 values for the decrease in significant wave height and decrease in wave energy are 0.74, and 0.65, respectively. This means that more vegetation at RBR 3 occupies the water column.

For stations RBR 2 and RBR 4, the RR is much lower compared to the RR at RBR 3, which means there is a lower percentage decrease in both significant wave height and wave energy. This is due to the Relative Roughness. RBR 3 is in the fully vegetated canopy, whereas RBR 2 is located on the marsh edge. The marsh edge has some vegetation or is often a bare stubbly surface, which means that at times, no vegetation is present to be submerged, and if there is any it is occupies a small fraction of the water column. In some instances, RBR 4 has water, which allows for some of the vegetation to be submerged. However, the impact of the topography could also be a factor that results in a decrease in both significant wave height and wave energy.

CHAPTER FIVE

DISCUSSION AND CONCLUSIONS

In this paper, we investigated how effective *Spartina alterniflora* is at attenuating wave energy over Neap/Spring tidal cycles and how its wave attenuation capacity varies with varying heights of the canopy and water depth. The results of our study show that vegetation height and water depth play an important role in dissipating wave energy and attenuating significant wave heights. Furthermore, the results show that where the water depth is less than 1 m, there is a greater reduction in significant wave height within the first 10 m of the transect, compared to where the water depth is greater than 1 m. For water depths less than 1 m, over 60% wave energy is dissipated within the first 10 m of the marsh, whereas for water depths greater than 1 m, between 50 and 72 % of the wave energy is dissipated at a much further distance of 50 m. If another threshold had been chosen, then we would expect different results of decrease in significant wave height and wave energy values.

Irrespective of the time of year or sampling period, vegetation attenuates wave height and dissipates wave energy. However, the efficiency at which this occurs is dependent on water depth. In both cases where water depth is greater than 1 m, and where water depth is less than 1 m, the mean significant wave height decreases from the marsh edge, advancing towards the vegetated section of the transect. Based on the results, over 60 % of wave energy is dissipated within the first 10 m of the marsh, for water depths less than 1 m (Figure 4.5a and Figure 4.5b). However, for water depths greater than 1 m, between 50 and 72 % of the wave energy is dissipated at a much further distance of 50 m.

The effectiveness of *Spartina alterniflora* canopy in dissipating wave energy also differs depending on RR. Vegetation properties have a great influence on wave dissipation. During powerful storms, stems that are more flexible stems tend to flatten, yet wave dissipation can still occur (Leonardi et al., 2019). It is evident that the presence of vegetation plays a vital role in wave dissipation. Vegetation provides a barrier or supplies bottom friction that dissipates wave energy (Möller et al, 2002). However, in some cases, as wave height increases, stem breakage can occur, which limits wave dissipation factors. Stem height, diameter, and flexibility of plant affects the amount of wave force it can withstand (Feagin et al., 2011). With increasing stem density and stem height throughout the deployment period, the results show that tall and dense vegetation is highly effective at dissipating wave energy (Foster-Martinez et al., 2018). The mean stem height values for RBR 2, RBR 3 and RBR 4 were recorded as 54.2 cm, 61.5 cm, and 46.0 cm, respectively. For the percentage decrease in significant wave height, the results show R^2 values of 0.26, 0.74 and 0.67 for RBR 2, RBR 3 and RBR 4, respectively (Figure 4.6.). The greatest decrease in significant wave height occurs at RBR 3 as it has the tallest vegetation. RBR 4 which is at the very end of the transect is at a much higher elevation compared to the three other instruments along the transect, hence, which means that less vegetation occupies the water column.

A study carried out by Möller et al., 2002, to investigate the wave dissipation over macro-tidal salt marshes also found that reduction in wave heights is most rapid over the most seaward 10 metres of permanent salt marsh vegetation. This is similar to the results from our study, where over 60 % of wave energy is dissipated within the first 10 metres of the marsh, for water depths less than 1 m.

Canopies that are submerged reduce flow and turbulence (Duarte et al., 2013). Our findings also show that the wave dissipation potential of salt marshes is highly influenced by the RR (Figure 4.6 and Figure 4.7). These findings are similar to a study carried out by Möller et al, 1999, in North Norfolk, England, to investigate the effectiveness of a meso- to macro-tidal open coast salt marsh at attenuating waves over a range of tidal and meteorogical conditions. Möller et al. (1999) found that the rates of wave energy dissipation over the salt marsh were significantly higher compared to those over a sand flat, with wave dissipation values of 82% and 29% respectively (Möller et al, 1999). This was due to the differences in water depth between the sand flat and the salt marsh (Möller et al, 1999). According to this study, the effectiveness of vegetation at wave energy dissipation increases with the percentage of the water column it occupies. i.e., as the canopy occupies more of the water column and the canopy becomes more submerged, the flow and turbulence are reduced even more (Duarte et al., 2013).

5.1. Limitations of the study and further recommendations

Given that the wave conditions are highly influenced by the wind currents, it is recommended that further studies focus on deploying a weather station at the site to ensure that wind conditions are monitored and recorded, allowing for the data to be included those in the overall analysis. It would also be vital to deploy another instrument within the transect. In our study, we deployed 4 instruments in a transect at 0 m, 5 m, 15m and lastly 50 m. However, we noticed that there was a much larger distance between RBR 3 and RBR 4, which created a data gap in our analysis. This would have helped us understand the impact of topography on the reduction of both significant wave height and wave energy. Although we deployed RBRX in the last two weeks of our study, at a 25 m distance from RBR 1, the data obtained during those two weeks, was insufficient to be included in our overall analysis.

Other recommendations include the extension of the study by commencing the deployment early Spring. The data obtained through a much longer deployment will allow for further analysis of how the effectiveness of *Spartina alterniflora* varies with the changes in vegetation characteristics, and wave conditions over a much larger time frame.

CHAPTER SIX

POTENTIAL APPLICATIONS

Consequently, our results also showed that tall and dense vegetation is highly effective at dissipating wave energy. To profit from the benefit of the presence of vegetation on salt marshes, it is recommended to promote salt marsh restoration and further investigate the effectiveness of *Spartina alterniflora* in attenuating wave energy, under different conditions such as storm conditions. Studies have found that the presence of vegetation cover is essential as it results in additional friction, which in turn enhances the wave dissipation over a salt marsh (Möller et al., 2002). The knowledge of the wave dissipation potential of salt marshes presents an opportunity for a cost-effective element of coastal protection schemes ((Möller et al., 2014; Rupprecht et al., 2017; Sutton-Grier et al., 2015). As salt marshes have the ability vertically adapt as the sea level rises, they play a vital role in coastal defence (Graham and Manning, 2007). Our research presents an opportunity for salt marshes to be included in quantitative flood risk assessments and adaptive coastal management. When investigating nature-based solutions to flooding, salt marshes can also be incorporated as a component (Vuik et al., 2016). However, prior to considering them as full alternatives for conventional flood defences, there is need to test their probability of failure according to engineering standards (Vuik et al., 2016).

Understanding the wave dissipation potential of salt marshes is important to help inform designs for marsh restorations and management plans (Moller et al., 2014). This study provides a step towards closing the knowledge gap in studies on coastal protection and how to build climate resilient communities and ecosystems through nature-based adaptation and implementation of natural infrastructure solutions, specifically within the Bay of Fundy (Virgin et al., 2020).

REFERENCES:

Allen, J. R. (2000). Morphodynamics of Holocene salt marshes: a review sketch from the Atlantic and Southern North Sea coasts of Europe. *Quaternary Science Reviews*, *19*(12), 1155-1231.

Amos, C. L., & Alföldi, T. T. (1979). The determination of suspended sediment concentration in a macrotidal system using Landsat data. *Journal of Sedimentary Research*, *49*(1), 159-173.

Ashall, L. M., Mulligan, R. P., van Proosdij, D., & Poirier, E. (2016). Application and validation of a three-dimensional hydrodynamic model of a macrotidal salt marsh. *Coastal Engineering*, *114*, 35-46.

Bouma, T. J., De Vries, M. B., Low, E., Peralta, G., Tánczos, I. V., van de Koppel, J., & Herman, P. M. J. (2005). Trade-offs related to ecosystem engineering: A case study on stiffness of emerging macrophytes. *Ecology*, *86*(8), 2187-2199.

Bowron, T., Neatt, N., van Proosdij, D., Lundholm, J., & Graham, J. (2011). Macro-tidal salt marsh ecosystem response to culvert expansion. *Restoration Ecology*, *19*(3), 307-322.

Bridges, T. S., Burks-Copes, K. A., Bates, M. E., Collier, Z. A., Fischenich, J. C., Piercy, C. D., ... & Vuxton, E. A. (2015). *Use of natural and nature-based features (NNBF) for coastal resilience*. Vicksburg: US Army Engineer Research and Development Center, Environmental Laboratory, Coastal and Hydraulics Laboratory.

Broome, S., Seneca, E., & Woodhouse, W. (1988). Tidal salt marsh restoration. *Aquatic Botany*, *32*(1-2), 1-22.

Byers, S. E., & Chmura, G. L. (2007). Salt marsh vegetation recovery on the Bay of Fundy. *Estuaries and Coasts*, 869-877.

Byers, S. E., & Chmura, G. L. (2014). Observations on shallow subsurface hydrology at Bay of Fundy macrotidal salt marshes. *Journal of Coastal Research*, *30*(5), 1006-1016.

Davidson-Arnott, R., Bauer, B., & Houser, C. (2019). *Introduction to coastal processes and geomorphology*. Cambridge university press.

Desplanque, C., & Mossman, D. J. (2004). Tides and their seminal impact on the geology, geography, history, and socio-economics of the Bay of Fundy, eastern Canada. *Atlantic Geology*, *40*(1).

Duarte, C. M., Losada, I. J., Hendriks, I. E., Mazarrasa, I., & Marbà, N. (2013). The role of coastal plant communities for climate change mitigation and adaptation. *Nature Climate Change*, *3*(11), 961-968.

Feagin, R. A., Irish, J. L., Möller, I., Williams, A. M., Colón-Rivera, R. J., & Mousavi, M. E. (2011). Engineering properties of wetland plants with application to wave attenuation. *Coastal Engineering*, *58*(3), 251-255.

Foster-Martinez, M. R., Lacy, J. R., Ferner, M. C., & Variano, E. A. (2018). Wave attenuation across a tidal marsh in San Francisco Bay. *Coastal Engineering*, *136*, 26-40.

Friedrichs, C. T., & Perry, J. E. (2001). Tidal salt marsh morphodynamics: a synthesis. *Journal of Coastal Research*, 7-37.

Graham, G. W., & Manning, A. J. (2007). Floc size and settling velocity within a Spartina anglica canopy. *Continental Shelf Research*, *27*(8), 1060-1079.

Grant, D. R. (1970). Recent coastal submergence of the Maritime Provinces, Canada. *Canadian Journal of Earth Sciences*, *7*(2), 676-689.

Jadhav, R. S., Chen, Q., & Smith, J. M. (2013). Spectral distribution of wave energy dissipation by salt marsh vegetation. *Coastal Engineering*, *77*, 99-107.

Koch, E. W., Barbier, E. B., Silliman, B. R., Reed, D. J., Perillo, G. M., Hacker, S. D., ... & Wolanski, E. (2009). Non-linearity in ecosystem services: temporal and spatial variability in coastal protection. *Frontiers in Ecology and the Environment*, *7*(1), 29-37.

Leonard, L. A., & Croft, A. L. (2006). The effect of standing biomass on flow velocity and turbulence in Spartina alterniflora canopies. *Estuarine, Coastal and Shelf Science*, *69*(3-4), 325-336.

Leonardi, N., Carnacina, I., Donatelli, C., Ganju, N. K., Plater, A. J., Schuerch, M., & Temmerman, S. (2018). Dynamic interactions between coastal storms and salt marshes: A review. *Geomorphology*, *301*, 92-107.

Möller, I., & Spencer, T. (2002). Wave dissipation over macro-tidal saltmarshes: Effects of marsh edge typology and vegetation change. *Journal of Coastal Research*, (36), 506-521.

Möller, I., Kudella, M., Rupprecht, F., Spencer, T., Paul, M., Van Wesenbeeck, B. K., ... & Schimmels, S. (2014). Wave attenuation over coastal salt marshes under storm surge conditions. *Nature Geoscience*, *7*(10), 727-731.

Möller, I., Spencer, T., French, J. R., Leggett, D. J., & Dixon, M. (1999). Wave transformation over salt marshes: a field and numerical modelling study from North Norfolk, England. *Estuarine, Coastal and Shelf Science*, *49*(3), 411-426.

Neumeier, U. (2005). Quantification of vertical density variations of salt-marsh vegetation. *Estuarine, Coastal and Shelf Science*, *63*(4), 489-496.

Pinsky, M. L., Guannel, G., & Arkema, K. K. (2013). Quantifying wave attenuation to inform coastal habitat conservation. *Ecosphere*, *4*(8), 1-16.

Rahman, T.; Sherren, K.; Manuel, P.; Rapaport, E. and D. van Proosdij. In Review. Characterizing Barriers to Nature Based Coastal Adaptation Approaches. *Wiley Interdisciplinary Reviews: Climate Change* Submitted March 24, 2020. Accepted with revisions July 18, 2020. Accepted with major revisions, Revisions submitted Aug 28, 2020.

Rupprecht, F., Möller, I., Evans, B., Spencer, T., & Jensen, K. (2015). Biophysical properties of salt marsh canopies—Quantifying plant stem flexibility and above ground biomass. *Coastal Engineering*, *100*, 48-57.

Rupprecht, F., Möller, I., Paul, M., Kudella, M., Spencer, T., Van Wesenbeeck, B. K., ... & Schimmels, S. (2017). Vegetation-wave interactions in salt marshes under storm surge conditions. *Ecological Engineering*, *100*, 301-315.

Sales Jr, R. F. M. (2009). Vulnerability and adaptation of coastal communities to climate variability and sea-level rise: Their implications for integrated coastal management in Cavite City, Philippines. *Ocean & Coastal Management*, *52*(7), 395-404.

Shepard, C. C., Crain, C. M., & Beck, M. W. (2011). The protective role of coastal marshes: a systematic review and meta-analysis. *PloS one*, *6*(11), e27374.

Singh, K., Walters, B. B., & Ollerhead, J. (2007). Climate change, sea-level rise and the case for salt marsh restoration in the Bay of Fundy, Canada. *Environments*, *35*(2), 71.

Sutton-Grier, A. E., Wowk, K., & Bamford, H. (2015). Future of our coasts: The potential for natural and hybrid infrastructure to enhance the resilience of our coastal communities, economies and ecosystems. *Environmental Science & Policy*, *51*, 137-148.

Van Proosdij, D., Lundholm, J., Neatt, N., Bowron, T., & Graham, J. (2010). Ecological re-engineering of a freshwater impoundment for salt marsh restoration in a hypertidal system. *Ecological Engineering*, *36*(10), 1314-1332.

Vandenbruwaene, W., Maris, T., Cox, T. J. S., Cahoon, D. R., Meire, P., & Temmerman, S. (2011). Sedimentation and response to sea-level rise of a restored marsh with reduced tidal exchange: Comparison with a natural tidal marsh. *Geomorphology*, *130*(3-4), 115-126.

Virgin, S. D., Beck, A. D., Boone, L. K., Dykstra, A. K., Ollerhead, J., Barbeau, M. A., & McLellan, N. R. (2020). A managed realignment in the upper Bay of Fundy: Community dynamics during salt marsh restoration over 8 years in a megatidal, ice-influenced environment. *Ecological Engineering*, *149*, 105713.

Vuik, V., Jonkman, S.N., Borsje, B. W., & Suzuki, T. (2016). Nature-based flood protection: The efficiency of vegetated foreshores for reducing wave loads on coastal dikes. *Coastal Engineering*, *116*, Urn: issn:0378-3839.

Vuik, V., Van Vuren, S., Borsje, B. W., van Wesenbeeck, B. K., & Jonkman, S. N. (2018). Assessing safety of nature-based flood defenses: Dealing with extremes and uncertainties. *Coastal engineering*, *139*, 47-64.

Willemsen, P. W., Borsje, B. W., Vuik, V., Bouma, T. J., & Hulscher, S. J. (2020). Field-based decadal wave attenuating capacity of combined tidal flats and salt marshes. *Coastal engineering*, *156*, 103628.

Wilson, E. K., Hill, P. S., van Proosdij, D., & Ruhl, M. (2017). Coastal retreat rates and sediment input to the Minas Basin, Nova Scotia. *Canadian Journal of Earth Sciences*, *54*(4), 370-378.

Zedler, J. B. (Ed.). (2000). Handbook for restoring tidal wetlands. *CRC press*.

APPENDIX:

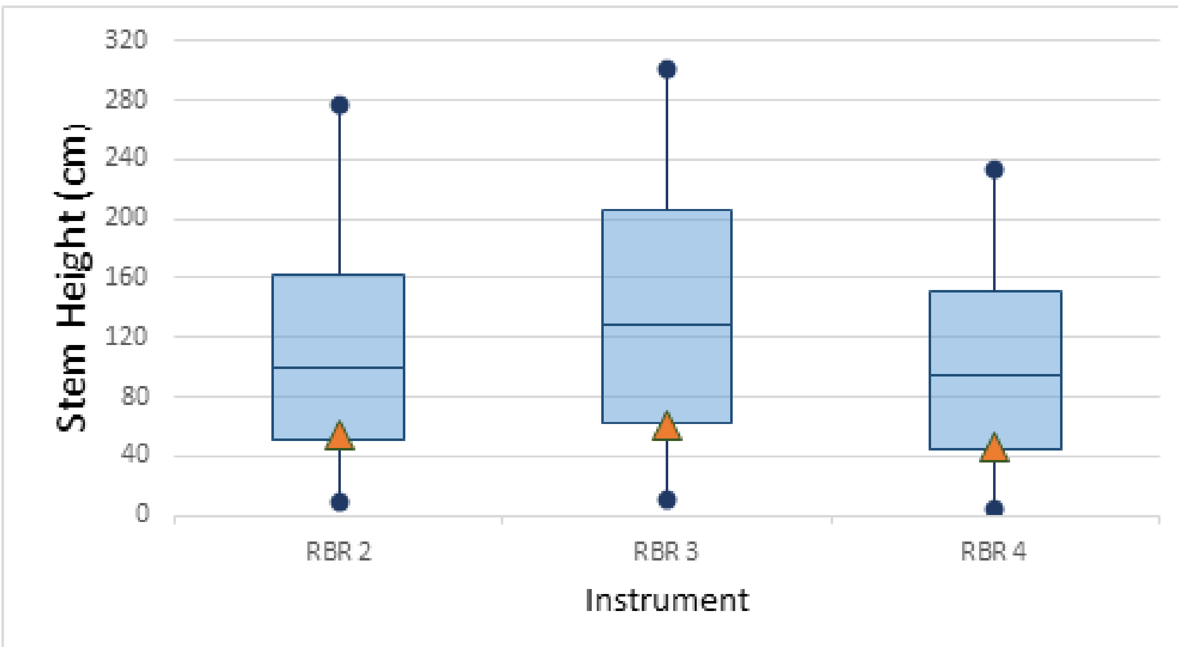

Figure A1. A box and whisker plot showing the stem height values recorded from June 18 to December 3, 2020. The orange triangle represents the mean values of 54.2 cm, 61.5 cm, and 46.0 cm at RBR 2, RBR 3 and RBR 4, respectively. Q1, Q2 and Q3 are shown above.

Table A1. Parameters measured by RBRs.

Depth	m
Sea pressure	dbar
Wave energy	J/m^2
Average wave period	s
Average wave height	m
Maximum wave period	s
1/10 wave height	m
Significant wave period	s
Tidal slope	m/h
Pressure	dbar
Temperature	°C

The RBR*duet*³ T.D|wave16 — temperature & pressure (RBR Ltd, Canada) instruments were programmed prior to deployment with the following settings:

Mode: Wave

Speed: 4Hz

Duration: 2048 therefore 8.5 minutes bursts

Interval: 10:00 min

Instrument altitude: 0.10 m

Mean Depth of Water: 2.0 m

Therefore Wave Bandwidth: 0.0020 to 0.4902 Hz

Wave periods: 2.04 to 512 seconds

All RBRs were programmed to start at 5.00 p.m.

The instruments were all deployed in the same configuration.

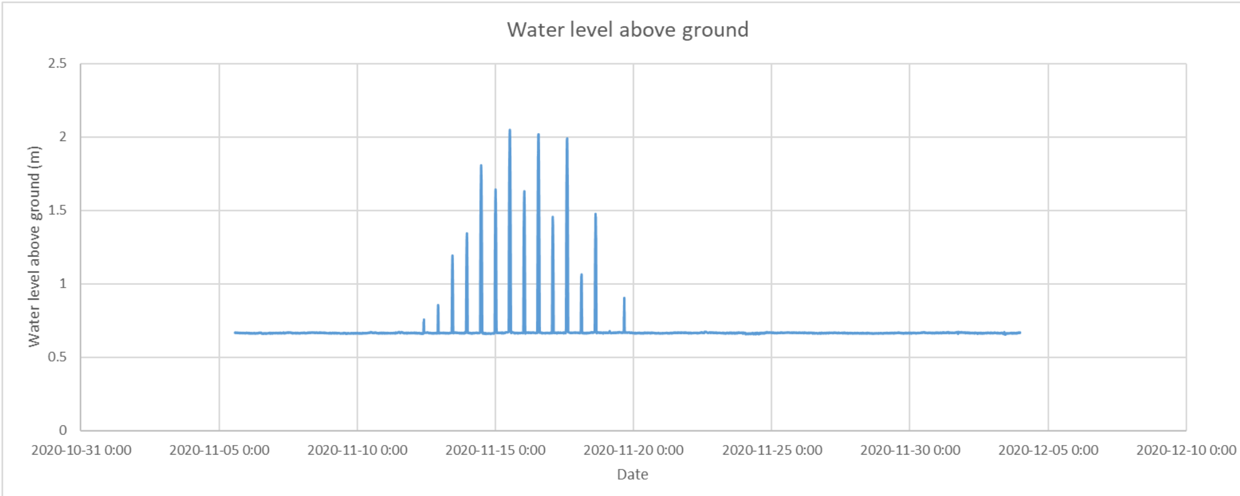

Figure A2. Water level above ground (m) from November 5th, 2020 to December 3rd, 2020

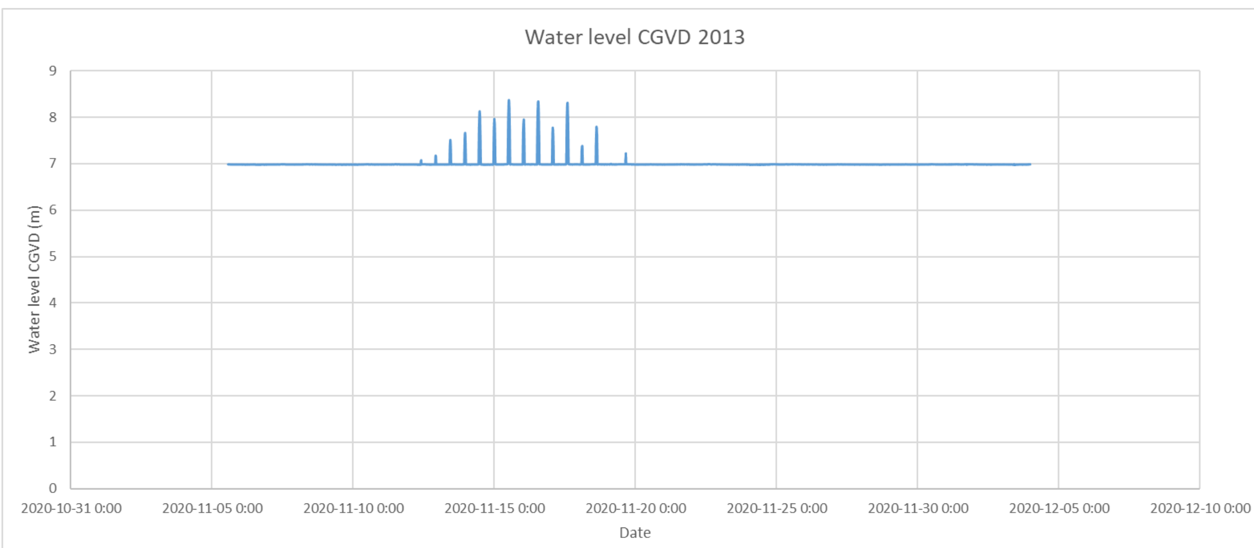

Figure A3. Water level CGVD (m) from November 5th, 2020 to December 3rd, 2020

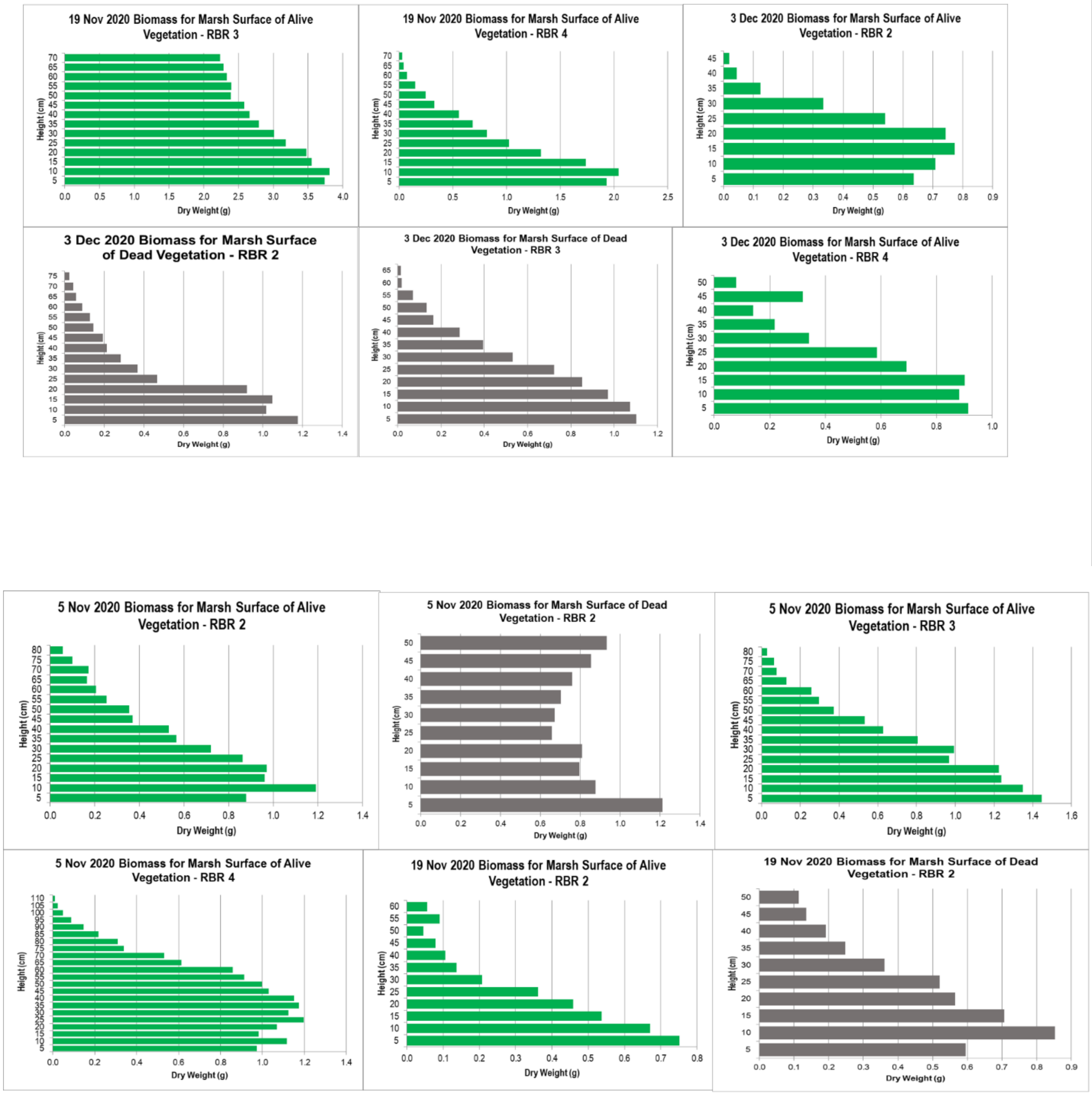

Figure A4. Aboveground biomass calculations on November 5, November 19 and December 3, 2020. Green represents alive, while grey represents dead aboveground biomass.